
JOINT INFERENCE OF DIFFUSION AND STRUCTURE IN PARTIALLY OBSERVED SOCIAL NETWORKS USING COUPLED MATRIX FACTORIZATION

Maryam Ramezani

Computer Engineering Department
Sharif University of Technology
maryam.ramezani@sharif.edu

Aryan Ahadinia

Computer Engineering Department
Sharif University of Technology
aryan.ahadinia@sharif.edu

Amirmohammad Ziaei

Computer Engineering Department
Sharif University of Technology
ziaei@ce.sharif.edu

Hamid R. Rabiee

Computer Engineering Department
Sharif University of Technology
rabiee@sharif.edu

ABSTRACT

Access to complete data in large-scale networks is often infeasible. Therefore, the problem of missing data is a crucial and unavoidable issue in the analysis and modeling of real-world social networks. However, most of the research on different aspects of social networks does not consider this limitation. One effective way to solve this problem is to recover the missing data as a pre-processing step. In this paper, a model is learned from partially observed data to infer unobserved diffusion and structure networks. To jointly discover omitted diffusion activities and hidden network structures, we develop a probabilistic generative model called "DiffStru." The interrelations among links of nodes and cascade processes are utilized in the proposed method via learning coupled with low-dimensional latent factors. Besides inferring unseen data, latent factors such as community detection may also aid in network classification problems. We tested different missing data scenarios on simulated independent cascades over LFR networks and real datasets, including Twitter and Memtracker. Experiments on these synthetic and real-world datasets show that the proposed method successfully detects invisible social behaviors, predicts links, and identifies latent features.

Keywords Social Network · Information Diffusion · Partially Observed Data · Network Structure · Matrix Factorization · Link Prediction · Cascade Completion · Bayesian Computation · Coupled Matrix Factorization

1 Introduction

Social networks are essential platforms for the interaction of people through an explicit link by following each other and an implicit connection by sharing information. The widespread use of social networks by increasing the number of users, the large number of interactions between them, and the amount of information propagation over these networks have led to a line of research focused on analyzing and modeling these networks. The target audience for the results of this research are either:

1. The owners of these platforms (e.g., Twitter, Instagram)
2. The third-party enterprises with customers who use these platforms (e.g., advertising companies, product providers, news analysts).

This paper focuses on solving the missing data problem for the latter community. In the context of large-scale social media, data collection is a massive, expensive, and time-consuming task for third-party companies. Typically, social datasets are provided for a limited period and include a subset of users for specific applications. In practice, having

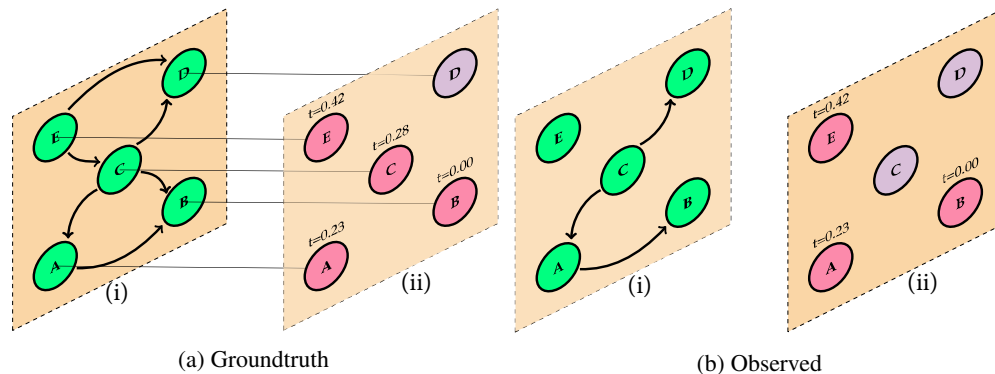


Figure 1: Our problem at a glance. A structural network is described by frame (i): If A follows B , there is a link from A to B . Frame (ii) focuses on diffusion behaviors, where pink-colored nodes indicate infected nodes with their time of infection. Part (b) contains the same frames as part (a), with missing data in each frame indicating partial observations. This paper aims to extract the complete data (a) by combining structural information (frame (i)) with diffusion information (frame (ii)) in the observed mode (b).

access to the complete data of a network is impossible even for a short period, and we often observe a partial subset of social data because of the following reasons:

1. API call restrictions: Most social network platforms provide public API for data access in well-defined formats and automatically trigger a rate-limiting mechanism. For example, Twitter, Instagram, and Facebook impose a rate limit on getting a user’s list of following/followers or posts,
2. Rate-limit for web crawler: Websites usually set a limited number of requests for fetching data per IP address. When a crawler scrapes the site, a temporary ban occurs when its request rate exceeds the predefined limit,
3. Sampling technique: Due to the large volume and variety of data in a network, sampling methods are used for prioritization. Depending on the sampling method, missing data arise through the collection process,
4. Protecting privacy: Statistics have shown that social network users’ private accounts and rates of private activities are steadily on the rise Vesdapunt and Garcia-Molina [2015]. Since web crawlers do not have access to the information of the private accounts, the collected dataset does not represent the complete data.

Although much research has been done on social network aspects, most do not consider the problem of missing data. Hence, the completeness assumption in those social network methods affects their performance on actual data. To alleviate this problem, some methods utilize a pre-processing algorithm on the input datasets to obtain a set with the least missing data to compensate for their completeness assumption. The main question is: How can we apply the existing methods to the original crawled data of social networks that contain missing data? In this paper, we try to provide an answer to this question for a specific type of data (graph-structured data with diffusion information) by proposing a probabilistic generative method called DiffStru.

A network can be modeled by a graph including users and their interactions. The activity of users in time is another data representing a phenomenon over a network named diffusion. Diffusion is usually known as a set of propagation processes called a cascade. A cascade transmits information from one user to another connected user in a network. A user is said to be infected in a cascade if it receives republished information from another user. In this context, infection time is the time of user activity in publishing or republishing information in a cascade. It is good to note that in most social platforms, the name of nodes and their infection time is the only accessible data from cascades and other additional data, such as the infection path and the trace of who infected who is unknown. While the cascade graph is not accessible, the partial sets of nodes and infection times in each cascade are available. These concepts in a social network like Twitter are: users having an account on Twitter can be modeled as nodes of a graph with directed links expressing following and follower relations between them. When a user tweets a piece of information, her/his followers will receive it, and the sequence of the tweet’s retweets will establish a cascade. A collection of cascades for different tweets forms diffusion.

Even if we consider a set of nodes in data collection and obtain the links between them for a time interval, we have some unobserved links due to the above-mentioned limitations. On the other hand, unobserved information in diffusion data appears as missing activity of nodes in each cascade. Fig. (1) illustrates the problem we are trying to solve. Given a limited period with a partially observed network graph structure and diffusion information containing the same set of

users, our goal is to complete the missing data.

We make the following assumptions:

1. We assume that the data are collected over a limited period, such that the network structure remains static (no new users join or leave the network), and a timestamp for the creation of the link is not available during that period. In addition, this assumption implies that the diffusion information collected during crawling is based on a static structure. Thus, the network links are also static, and the data is fixed during interactions. On the other hand, a cascade has a limited lifespan. It spreads over hours to days, which means the sequence from beginning to end is usually fixed within a specific data collection interval.
2. We are not interested in hidden nodes with no global or local signals in structure or diffusion data. However, we can somewhat handle users with private accounts. Although we cannot observe their profiles and activities, we can obtain their interactions from the list of following/followers of their visible neighbors. Therefore, the one-step neighbors of visible users are not hidden, while we are not engaged in any hidden neighbors of private users.
3. We consider that the source and mediators of an information dissemination process are internal network factors and any external agents are ignored.

As mentioned before, incomplete data in the collected set from a social network is inevitable, and missing data can significantly affect the difference between the output of methods and what happens in the real world Belák et al. [2016]. Considering the missing data in two levels of structure and diffusion simultaneously makes the data inference challenging. Here, we try to make the inference tractable by selecting the appropriate distributions on the data. We present a novel generative model for jointly inferring the partial network structure and the information diffusion.

The contributions of this paper are as follows:

- Tackling the problem of missing data **both in diffusion and structure** in real-world social datasets by proposing a new probabilistic generative model to jointly discover the hidden links of network structure and omitted diffusion activities.
- Investigating structure and diffusion joint properties via probabilistic matrix factorization.
- Inferring the missing links of a network structure and the missing activities of nodes when a partial graph and a set of cascades with missing data are observable.
- Inferring the diffusion behavior of users even when the user page is private and we have no information about his activities.
- Demonstrating that the low-dimensional representations for characteristics of users and cascades during the inference of DiffStru can be widely used in embedding and classification problems.

The rest of the paper is organized as follows: First, in Section (2), we present a review of social research related to partially observed data that motivates the paper. In Section (3), we review the related work, while Section (4) contains the paper notations, definitions, and problem statement. We present the proposed model in Section (5). In Section (6), we examine the empirical results on synthetic and real-world datasets. Finally, we present the conclusions by discussing future work in Section (7).

2 Historical Background and Motivation

Partially observed data has received enormous attention in previous studies of social networks. In the scope of this paper, social data is divided into two classes: **structure** networks (nodes and links between them) and **diffusion** (cascades propagation over a network). Missing data can occur in each of these two classes.

Regarding history, missing data was first raised for structural network data, a long-standing research track known as link prediction. The main goal of this track is to find the missing links using observed interactions without considering diffusion information. Over the years, different assumptions and methods have been employed to solve the link prediction problem.

Over time, due to the focus on the correlation between the diffusion process and network structure, both data classes have been considered together. In contrast, missing data is assumed at either the diffusion or structure class (but not both). For missing data at the diffusion class, one of the first attempts to analyze partially observed cascades was Sadikov et al. [2011]. As long as the structural network is complete, the model attempts to estimate the properties of a whole cascade by using incomplete missed cascade samples. In missing data at structure class, Belák et al. [2016]

examines the characteristics of the diffusion process over partial network structures. It attempts to infer the truth of cascade broadcasts occurring in the underlying network.

In the later years, different studies were published on the study of dynamic-on (diffusion) and dynamic-off (structure) networks Antoniadou and Dovrolis [2015], Farajtabar et al. [2017]. The diffusion process affects the evolution of a network, and the change in the network impacts the life cycle of diffusion processes as well. Therefore, dynamics on and off affect each other Weng et al. [2013]. Paper Zhang et al. [2015] proposes a time-delayed model for new link formation based on pre-existing links over time. Another paper finds new links by classical link prediction methods, then applies diffusion processes to new networks and evaluates and analyzes evolved networks' structural and diffusion processes Vega-Oliveros et al. [2019].

Table (1) categorized different views of data missing occurrence in structure and diffusion class. Paying attention to each of them leads to solving different social network problems:

- **Complete diffusion with partially structure network**
When a network is incomplete, it means some nodes and links are missing. As a result, forecasting and optimizing the diffusion process based on this partially observed network is not the same in reality. Estimating the cascade's influence on the unobserved part of the network is necessary. Seed selection for influence maximization is an application of this problem Belák et al. [2016], Sumith et al. [2018].
- **Complete diffusion with no structure network**
Network inference problems fall into this category. When the interaction topology of a network is entirely unreachable, an inference approach is put forward using visible independent measurements Newman [2018a]. An observational measurement could be the signals received from nodes or the cascades over the network Gomez-Rodriguez et al. [2012, 2013], Rodriguez et al. [2014], Ramezani et al. [2017], Ji et al. [2020], Huang et al. [2019], Gomez Rodriguez et al. [2013], Tahani et al. [2016], Woo et al. [2020], Ghonge and Vural [2017], Newman [2018b], Kefato et al. [2019].
- **Partially diffusion with complete structure network**
In the case of a complete graph of the network but incomplete information propagation, we have different diffusion problems, which include:
 - (1) Identifying the future infected nodes in a cascade sequence by observing the incomplete and primary parts of a cascade sequence Wang et al. [2017], Yang et al. [2019], Wang et al. [2017], Islam et al. [2018], Yang et al. [2019], Wang et al. [2022a], Najjar et al. [2012], Sun et al. [2022],
 - (2) Discovering the source of diffusion Farajtabar et al. [2015], Shi et al. [2022],
 - (3) Detecting missing parts of the cascade, such as nodes that were missed or infection times that were not observed Sundareisan et al. [2015],
 - (4) Estimating the properties of complete cascades based on partially sampled diffusion Sadikov et al. [2011].
- **Partially diffusion with no structure network**
Based on the few first windows of the cascade, some works attempt to predict the future size of the cascade without knowing how the nodes interact Chen et al. [2022] or ranking the next infected nodes Chen et al. [2022], Yuan et al. [2021], Wang et al. [2022b, 2021]. The researchers also try to model cascade propagation.
- **No diffusion data with complete structure network**
Modeling the pattern and path of a cascade over a network is the purpose of this category Saito et al. [2008].
- **No diffusion data with partially structure network**
The purpose of this category is to recover missing parts of a network. The omitted part can include nodes, and links Kim and Leskovec [2011]. There are numerous proposed models to predict lost links in a network when all nodes and some links are present Kim and Leskovec [2011], Rafailidis and Crestani [2016], Masrour et al. [2015], Airoidi et al. [2008], Wang et al. [2018], Mutlu and Oghaz [2019], Menon and Elkan [2011], Li et al. [2016], Jia et al. [2015], Wai et al. [2022], Tang [2023], Chai et al. [2022].
- **Partially diffusion with partially structure network**
According to our knowledge, there has been no prior research that specifically addresses the goals of this category. This paper aims to provide a method for simultaneous inference from cascade sequences and graph links when both have missing data.

Currently, there is no previous work that is precisely related to the goals of the proposed method. It is worth noting that the works without considering partial observations, such as graph embedding or networks evolving over time, are not properly grounded in the literature of this paper. Also, one of the advantages of this paper is correcting the omitted data of diffusion against inferring the missing links, which are outside the scope of those works.

Table 1: Classification of studies on diffusion process and network structure dimensions from the perspective of Complete (C) and Partial (P) data. (N) stands for Not considering that dimension.

		Structure		
		C	P	N
Diffusion	C	–	diffusion estimation	structure inference
	P	cascade prediction source detection missing detection	focus of this paper	cascade prediction
	N	diffusion modeling	link prediction network completion	–

3 Related Work

In this section, we summarize the related works with the assumption of incomplete data, either in structure or diffusion data, into three categories: "link prediction," "network inference," and "cascade correction and prediction."

Link prediction. Link prediction and network completion are two famous problems for solving missing data in structural networks. KronEM predicts missing nodes and links by combining an Expectation-Maximization (EM) approach with the Kronecker model of graphs Kim and Leskovec [2011]. Some works utilize side information such as node attribute Rafailidis and Crestani [2016] or pairwise similarity between nodes Masrouf et al. [2015] to complete the network.

All nodes are visible in the link prediction works, while some links are omitted. There are numerous link prediction methods, including traditional supervised and unsupervised learning methods, probabilistic stochastic block model Airolidi et al. [2008], matrix or tensor factorization Wang et al. [2018], locally-based algorithms, and deep learning based approaches Mutlu and Oghaz [2019]. Although many link prediction methods exist, we only refer to those utilizing diffusion information to obtain additional information or matrix factorization to make their prediction.

Menon and Elkan [2011] utilizes a link prediction matrix factorization with features of nodes to predict unobserved links. Li et al. [2016] employs diffusion features such as interactive activities of nodes in cascades against topology features for link prediction. Link prediction in Jia et al. [2015] is modeled with matrix factorization using the similarity of retweeting information between pairs of users. In addition to predicting a link, paying close attention to the partially observed graph is critical for recognizing the community involved Wai et al. [2022].

In LCPA Chai et al. [2022], a maximum likelihood method was proposed to estimate structure networks by perturbing the adjacency matrix iteratively and correcting it. A partial binary structure network adjacency matrix with complete binary attribute information of nodes is used in JWNMF Tang [2023]. It proposes a non-negative matrix factorization method using two binary adjacency and attribute matrices sharing a topological hidden factor matrix.

Network inference. The goal is to infer the links of the underlying network using a set of cascades. For this purpose, Netrate Rodriguez et al. [2014] solves a convex optimization, DANI Ramezani et al. [2017] employs maximum likelihood while preserving the structural features of the network, and REFINE Kefato et al. [2019] utilizes neural network and T-SVD for feature selection from nodes participating in different cascades to infer links between nodes that have similar embedding. Other attempts have been made to network inference, from static assumption requiring time stamp Gomez-Rodriguez et al. [2012, 2013], Rodriguez et al. [2014], Ji et al. [2020], Ramezani et al. [2017], Kefato et al. [2019] or without infection time Huang et al. [2019] to dynamic inference Gomez Rodriguez et al. [2013], Tahani et al. [2016]. Woo et al. [2020] uses a base graph and complete cascade for estimating the graph path of diffusion iteratively. As a step towards using prior knowledge, some works employ in-degree distribution for nodes Ghonghe and Vural [2017] and measurements such as pathways, network properties, and information about the links or nodes Newman [2018b].

Cascade correction and prediction. If the initial and incomplete parts of the cascade are observed, how can the future infected nodes be identified? In specific, the LSTM architecture is used for predicting the next node in a cascade with the help of a complete network structure Wang et al. [2017], estimating the next node Yang et al. [2019], Yang et al. [2019], Sun et al. [2022] or finding the next infection time with the ranking of nodes as the next infection step Wang et al. [2017], Islam et al. [2018]. If a propagation tree is available, Kim et al. [2022] uses the partial subgraphs to learn the representation of the full graph. NetFill finds the missing infected nodes and source of diffusion by observing incomplete and noisy cascades by proposing a model based on a Minimum Description Length (MDL) Sundareisan et al. [2015].

To the best of our knowledge, none of the existing research incorporates simultaneous joint structure and diffusion data to solve the missing data problem. However, they attempt to recover the missing parts of both separately. This paper proposes the DiffStru method, which will be discussed in more detail in the following sections. DiffStru is more accurate than previous link prediction works because it uses structure and diffusion information to detect missing links simultaneously. Furthermore, DiffStru can solve more tasks than link prediction due to its ability to learn latent factors. If missing data occur in cascades, the network inference methods will perform less accurately than DiffStru. Moreover, DiffStru can infer the missing information of diffusion during the cascade sequence, while diffusion prediction methods are only used for predicting future infections. Meanwhile, DiffStru can be improved by decreasing its sensitivity to network density and considering the dynamic nature of the network structure.

4 Modeling Information Diffusion and Network Structure

This section first introduces the notations and definitions used in the paper. Then, we state the joint inference problem of diffusion networks and structure from partially observed data.

We identify matrices, vectors, and scalars by uppercase bold-faced ($\mathbf{X} \in \mathbb{R}^{p \times q}$), lowercase bold-faced ($\mathbf{x} \in \mathbb{R}^{p \times 1}$) and normal lowercase (x) letters, respectively. All vectors are column vectors, and x_i is the i -th element of vector \mathbf{x} . Similarly, $\mathbf{X}_{.j}$ is the j -th column, \mathbf{X}_i is the i -th row \mathbf{X} , and \mathbf{X}_{ij} is the entry in the i -th row, and j -th column of \mathbf{X} . The $m \times m$ identity matrix is denoted by \mathbf{I}_m . $\mathbf{X}^T \in \mathbb{R}^{q \times p}$ returns the transpose of a matrix and $\text{vec}(\mathbf{X}) \in \mathbb{R}^{pq \times 1}$ is the linear operator flattening all the columns of the matrix to a column vector. For matrices $\mathbf{X} \in \mathbb{R}^{p \times q}$ and $\mathbf{Y} \in \mathbb{R}^{r \times s}$, $(\mathbf{X} \otimes \mathbf{Y}) \in \mathbb{R}^{pr \times qs}$ is referred to the Kronecker product of two matrices. If $p = r$ and $q = s$, then $(\mathbf{X} \circ \mathbf{Y}) \in \mathbb{R}^{p \times q}$ denotes the Hadamard product (elementwise). Table (2) summarizes the notations we use in the proposed method.

We model a static social network with graph $\mathbb{G} = (V, E)$ where V represents N nodes (users of the network), $N = |V|$, and E indicates the set of edges between nodes. Link E_{ij} is formed from the relationship of node i to node j . These edges represent directed and unweighted interactions ($E_{ij} \neq E_{ji}$) without considering the self-links. Suppose $\mathbf{G} \in \{0, 1\}^{N \times N}$ is the corresponding asymmetric adjacency matrix of \mathbb{G} . Since the links of network graph \mathbb{G} are not fully observable, the available structure of a network is a sub-graph $\hat{\mathbb{G}} = (V, \hat{E}) \subseteq \mathbb{G}$. Let $\hat{\mathbf{G}}$ be a $N \times N$ binary adjacency matrix where the set of one value entries $\Omega^+ = \{(i, j) : \hat{\mathbf{G}}_{ij} = 1\}$ denotes existing observed links of the network. Ω^- represents the missing links, while it may not surely mean to imply that there is no link. For each entry $(i, j) \in \Omega^-$, we may have $\mathbf{G}_{ij} = 1$ or $\mathbf{G}_{ij} = 0$ in the oracle network.

In addition to the network structure, we have a set of information diffusion cascades \mathbb{C} among the users represented by a matrix $\mathbf{C} \in \mathbb{R}^{N \times M}$. By denoting the overall spread of each information as cascade c_j ; the element $\mathbf{C}(v_i, c_j) = t_{ij}$ represents that cascade c_j reached the user v_i and infected it at hit time $t_{ij} \in [0, T] \cup \infty$, where ∞ used for users that are not infected by c_j during the observation window $[0, T]$. We also assume that hit time is set to zero at the beginning of each cascade, and the cascade cannot infect each node more than once during its lifetime. A piece of information j propagates over the structure network by transmitting through the links from an infected node to an uninfected node. Each cascade can be expressed as a $N \times 1$ vector $(\mathbf{C}_{.j})$. Since a contagion does not reach all N observed network users, we are faced with a sparse vector for each cascade. Let $\hat{\mathbf{C}}_{.j}$ be the observed vector for cascade j , which contains only a subset of the infected users with their hit times. Formally, $\Gamma_j^+ = \{(i) : \mathbf{C}_{ij} \in \mathbb{R}_+ \wedge \hat{\mathbf{C}}_{ij} = \mathbf{C}_{ij}\}$ is a set of indices of the observed entries. The state of other nodes of the network $\Gamma_j^- = \{V \setminus \Gamma_j^+\}$ is hidden from us, while in the ground truth of the diffusion process, they may be infected or legitimate uninfected nodes. By aggregating all the observed vectors of M different cascades in a matrix $(\hat{\mathbf{C}})$, the mask matrix for partially observable knowledge of diffusion can be represented with $\mathbf{\Gamma} \in \{0, 1\}^{N \times M}$ which is a mapping from the collection of M vector indices $(\Gamma_{j=1, \dots, M}^+$ and $\Gamma_{j=1, \dots, M}^-)$ to a matrix space.

The problem we want to solve is:

Given: The partially observed network structure matrix $\hat{\mathbf{G}}$ and information diffusion matrix $\hat{\mathbf{C}}$.

Goal: Recover the non-observed links of a network by estimating matrix $\hat{\mathbf{G}}$ and obtain the approximated hit time of unobserved users of the network who are interacting hiddenly in diffusion processes with discovering matrix $\hat{\mathbf{C}}$.

Our Approach: Since our goal is to recover the hidden entries of two partially observed matrices, it can be modeled like a matrix completion problem. Matrix factorization is a prevalent and effective technique for matrix completion problems by approximating a given matrix $\mathbf{S} \in \mathbb{R}^{m \times n}$ as a product of two low-rank latent factor matrices $\mathbf{Q} \in \mathbb{R}^{m \times r}$ and $\mathbf{H} \in \mathbb{R}^{r \times n}$ with a constraint on $r \ll \min(m, n)$, such that $\mathbf{S} \approx \mathbf{Q}\mathbf{H}$. The latent factors \mathbf{Q} and \mathbf{H} are r Dimension representation matrices and can be interpreted as embedding for rows and columns of \mathbf{S} . These factors can be learned

Table 2: Major notations and symbols used for DiffStru

Symbol	Description
N, M	number of users, cascades
$\mathbb{G}, V, E, \mathbf{G}$	network graph, set of nodes, set of edges (links), adjacency matrix
$\mathbf{C}, \hat{\mathbf{G}}$	$N \times M$ original diffusion matrix, $N \times N$ original structure matrix
$\mathbf{\Gamma}$	binary $N \times M$ mask matrix for partially observable knowledge of diffusion
$\mathbf{\Omega}$	binary $N \times N$ mask matrix for the partially observed structure of the network
$\hat{\mathbf{C}}, \hat{\mathbf{G}}$	observed diffusion matrix, observed structure matrix
D	dimension of latent low-rank factorize matrices
$f(\cdot)$	logistic sigmoid function
Ξ	$N \times N$ binary latent auxiliary variable for structure graph
\mathbf{R}	$N \times N$ stochastic auxiliary variable
$\mathbf{W}_Y, \mathbf{W}_U, \mathbf{W}_X$	covariance $M \times M, N \times N, N \times N$ matrices between pair of cascades, nodes
μ_{Ξ}	conjugate Beta prior for observing pair of nodes
α_1, α_2	hyper-parameters of a conjugate Beta prior assigned to the parameter μ_{Ξ}
σ_C, σ_R	variance parameters for Gaussian distribution of \mathbf{C}, \mathbf{R}
δ_0	dirac delta distribution at zero
\mathbf{P}	$N \times M$ infection probability of the nodes in cascades matrix
\mathbf{A}	$N \times N$ infection transfer matrix between each nodes
$\mathbf{\Pi}$	$N \times M$ binary hyper-parameter for diffusion information
$\mathbf{X}, \mathbf{Y}, \mathbf{U}$	$D \times N$ User, $D \times M$ Cascade, $D \times N$ Factor latent features
$\mathcal{N}, \mathcal{RN}$	Normal, Rectified Normal distribution
Ber, Beta, \mathcal{PG}	Bernoulli, Beta, Polya-gamma distribution
\mathcal{N}_t	Multivariate distribution for t dimension vector
\mathcal{MN}_{tq}	$t \times q$ Matrix Gaussian distribution
\otimes, \circ	kroncker product, Hadamard product (elementwise)
vec	linear operator flattening all the columns of the matrix to vector

even if \mathbf{S} is partially observed by minimizing the reconstruction error for the observed entries to recover the full \mathbf{S} Lee and Seung [2001].

We start from the idea that a node infection can signify how the nodes interact with each other in the network structure. However, the links between users can impact the diffusion process. As shown in Fig. (2), a network structure includes a set of users and social links between them while the information propagates among these users. A user would receive information if one of his friends (a user with whom he has a link to him) posted or reposted it. In conclusion, the diffusion process can reflect and drive the network's structure, demonstrating that two matrices \mathbf{G} and \mathbf{C} correlate. We will model this correlation property by sharing the same latent factors between \mathbf{G} and \mathbf{C} . Therefore, the unobserved entries of $\hat{\mathbf{G}}$ and $\hat{\mathbf{C}}$ matrices can be estimated using the coupled matrix factorization method.

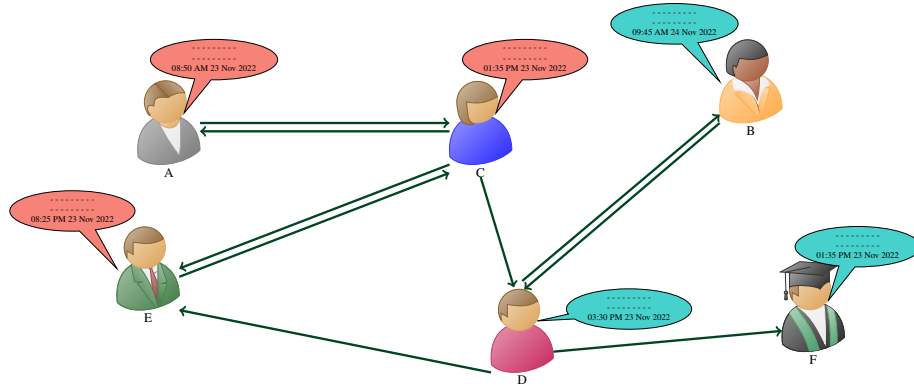


Figure 2: This illustrates the relationship between partially observed diffusion information and network structure. A link from "D" to "E" means D is following E, so E is the followee, and D, the follower monitor his post.

5 Proposed Method

This section presents the proposed model framework and how to infer the latent factor matrices.

5.1 Model Framework

The structural network \mathbf{G} is a Bernoulli distribution with a stochastic auxiliary variable \mathbf{R}_{ij} in the latent feature space:

$$\begin{aligned} \mathbf{G}_{ij} &= \text{Ber}(f(\mathbf{R}_{ij})) \\ \mathbf{R}_{ij} &= \mathbf{X}_i^T \mathbf{U}_{:j} + \varepsilon_{ij} \quad \varepsilon_{ij} \sim \mathcal{N}(0, \sigma_R^2) \end{aligned} \quad (1)$$

where $f(t) = \frac{1}{1 + e^{-t}}$ is the logistic sigmoid function. As shown in Fig. (3), \mathbf{R}_{ij} is constructed using Gaussian distribution with low-rank matrices $\mathbf{X} \in \mathbb{R}_+^{D \times N}$ and $\mathbf{U} \in \mathbb{R}^{D \times N}$ that represent user-specific and factor specific latent features, respectively. In order to limit the range of \mathbf{R}_{ij} to $[0, 1]$, a logistic sigmoid function $f(\cdot)$ is used. The Bernoulli distribution, which has 0 and 1 samples., is applied

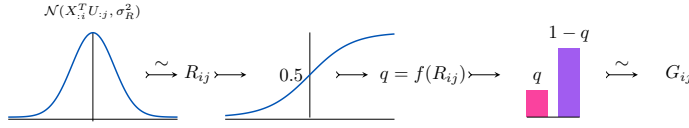


Figure 3: Mathematical Diagram of the generalized linear model for estimating the underlying link existence (\rightsquigarrow means sampling from the left distribution).

A binary latent auxiliary variable Ξ is employed as a link observer variable to express \mathbf{G} , which takes binary values.

- $\Xi_{ij} = 0$ means that we did not observe \mathbf{G}_{ij} (link existence between nodes v_i and v_j has not been investigated), so $\hat{\mathbf{G}}_{ij} = 0$.
- $\Xi_{ij} = 1$ implies that \mathbf{G}_{ij} was observed and based on (i, j) included in E_{ij} ($\mathbf{G}_{ij} = 1$) or not $\mathbf{G}_{ij} = 0$, $\hat{\mathbf{G}}_{ij}$ takes one or zero values, respectively.

While \mathbf{G}_{ij} is conditional on the value of Ξ_{ij} , the distribution function of \mathbf{G}_{ij} can be modeled as a mixture of two distributions with mixing weight Ξ_{ij} . The two components of \mathbf{G}_{ij} are assumed to be a Bernoulli distribution with a probability of success $f(\mathbf{R}_{ij})$ and a Dirac delta distribution at zero:

$$\mathbf{G}_{ij} \sim \Xi_{ij} \text{Ber}(f(R_{ij})) + (1 - \Xi_{ij}) \delta_0 \quad (2)$$

We consider the Bernoulli distribution for latent auxiliary variable $\Xi_{ij} \sim \text{Ber}(\mu_\Xi)$. By assuming equal probability for observing all pairs of nodes (v_i, v_j) that $i, j \in V, i \neq j$, a conjugate Beta prior with hyper-parameters α_1 and α_2 are assigned to the parameter $\mu_\Xi \sim \text{Beta}(\alpha_1, \alpha_2)$.

The cascade matrix \mathbf{C} can be modeled as:

$$\mathbf{C}_{ij} = \mathbf{X}_i^T \mathbf{Y}_{:j} + \eta_{ij} \quad \eta_{ij} \sim \mathcal{N}(0, \sigma_C^2) \quad (3)$$

where $\mathbf{X} \in \mathbb{R}_+^{D \times N}$ and $\mathbf{Y} \in \mathbb{R}_+^{D \times M}$ are low-rank matrices representing the user and cascade latent features with nonnegative entries, and η_{ij} denotes the residual noise sampled independently from zero-mean Gaussian distribution with variance σ_C^2 . The stochastic modeling of the hyper-parameter matrix $\mathbf{\Pi}$ as an observer for \mathbf{C} leads to an impossible inference model. Therefore, we resort to a deterministic model. The hyper-parameter $\mathbf{\Pi}_{ir}$ indicates that we have observer knowledge about the infection of node v_i in cascade c_r or not. Fig. (4) shows the generative Bayesian probabilistic representation of the proposed method for jointly inferring the Diffusion and Structure of the network called "DiffStru."

Our basic idea for joint inference is to incorporate the shared latent factor \mathbf{X} between network structure and diffusion matrices and choose the suitable prior distributions for considering the side information.

When a user account is private, no information about his diffusion behavior is available; hence, the corresponding rows of latent factors will be empty. However, we can handle these empty rows of matrices by integrating the side information as prior knowledge for capturing the correlation between users or cascades. Here, a zero-mean multivariate Gaussian distribution is employed as a conjugate prior of U as $\mathbf{U}_d \sim \mathcal{N}_N(0, \mathbf{W}_U)$ and X and Y are drawn from a rectified

multivariate Gaussian prior with zero mean: $\mathbf{X}_d \sim \mathcal{RN}_N(0, \mathbf{W}_X)$ and $\mathbf{Y}_d \sim \mathcal{RN}_M(0, \mathbf{W}_Y)$ for supporting nonnegative constraints. We exploit the diffusion and topological metrics as prior distributions for each row of the latent matrices \mathbf{Y}_d , \mathbf{U}_d , and \mathbf{X}_d , with covariance matrices \mathbf{W}_Y , \mathbf{W}_U , and \mathbf{W}_X , respectively. Each element of full covariance matrices $\mathbf{W}_Y \in \mathbb{R}^{M \times M}$ ($\mathbf{W}_U \in \mathbb{R}^{N \times N}$ or $\mathbf{W}_X \in \mathbb{R}^{N \times N}$) in these distributions capture the relationship between the pair of cascades (users) and also the correlation between different features of a cascade (user). These covariance matrices will apply the covariances between rows and columns of matrices in the priors Zhou et al. [2012]. We will show later in Section (6.4) how to initialize these covariances. The distributions are expressed as Algorithm (1).

Algorithm 1: Generative process for DiffStru graphical model

```

1  $\mu_{\Xi} \sim \text{Beta}(\alpha_1, \alpha_2)$ 
2  $\mathbf{Y}_d \stackrel{iid}{\sim} \mathcal{RN}_M(0, \mathbf{W}_Y), \forall d = 1, \dots, D$ 
3  $\mathbf{X}_d \stackrel{iid}{\sim} \mathcal{RN}_N(0, \mathbf{W}_X), \forall d = 1, \dots, D$ 
4  $\mathbf{U}_d \stackrel{iid}{\sim} \mathcal{N}_N(0, \mathbf{W}_U), \forall d = 1, \dots, D$ 
5 foreach user  $i = 1, \dots, N$  do
6   foreach user  $j = 1, \dots, N$  do
7      $\Xi_{ij} \stackrel{iid}{\sim} \text{Ber}(\mu_{\Xi})$ 
8      $\mathbf{R}_{ij} \stackrel{iid}{\sim} \mathcal{N}(\mathbf{X}_{:i}^T \mathbf{U}_{:j}, \sigma_R^2)$ 
9      $\mathbf{G}_{ij} \stackrel{iid}{\sim} \Xi_{ij}(\text{Ber}(f(\mathbf{R}_{ij}))) + (1 - \Xi_{ij})(\delta_0)$ 
10  end
11  foreach cascade  $r = 1, \dots, M$  do
12     $\mathbf{C}_{ir} \stackrel{iid}{\sim} \Pi_{ir}(\mathcal{N}(\mathbf{X}_{:i}^T \mathbf{Y}_{:r}, \sigma_C^2))$ 
13  end
14 end

```

In the general formulation based on the graphical model in Fig. (4), the joint distribution over the observed, latent, and auxiliary random variables given the hyper-parameters $\Theta = \{\mathbf{W}_Y, \mathbf{W}_X, \mathbf{W}_U, \alpha_1, \alpha_2, \sigma_C^2, \sigma_R^2, \mathbf{\Pi}\}$ is given by:

$$\begin{aligned}
 P(\mathbf{X}, \mathbf{U}, \mathbf{Y}, \mathbf{R}, \mathbf{\Xi}, \mu_{\Xi}, \mathbf{G}, \mathbf{C} | \Theta) &= \prod_{i=1}^N \prod_{j=1}^M (\mathcal{N}(\mathbf{R}_{ij} | \mathbf{X}_{:i}^T \mathbf{U}_{:j}, \sigma_R^2) \times [\mathcal{N}(\mathbf{C}_{ij} | \mathbf{X}_{:i}^T \mathbf{Y}_{:j}, \sigma_C^2)]^{\mathbf{\Pi}_{ij}} \\
 &\times [\text{Ber}(\mathbf{G} | f(\mathbf{R}_{ij}))]^{\mathbf{\Xi}_{ij}} \times \text{Ber}(\mathbf{\Xi}_{ij} | \mu_{\Xi}) \text{Beta}(\mu_{\Xi} | \alpha_1, \alpha_2)) \times \prod_{d=1}^D (\mathcal{N}_N(\mathbf{U}_d | 0, \mathbf{W}_U) \\
 &\times \mathcal{RN}_M(\mathbf{Y}_d | 0, \mathbf{W}_Y) \times \mathcal{RN}_N(\mathbf{X}_d | 0, \mathbf{W}_X))
 \end{aligned} \tag{4}$$

We should learn the posterior distribution to estimate the unobserved data using a Bayesian approach. A posterior with an intractable integral will be obtained using Bayes's rule. For approximating these integrals, the MCMC algorithm is a common approximation approach that tries to obtain a sufficient number of samples of the target distribution for a dependable inference Carlo [2004].

5.2 Model Inference

There are various ways to sample a distribution. In this case, we use the Gibbs method as an MCMC technique by iterative sampling one variable from a conditional distribution with fixing the remaining variables. In each iteration, all random variables are updated based on the previous value of others. We randomly initialize the values of random variables. To minimize the effect of random initialization, we should drop the first early samples, which is known as choosing the sufficient burn-in period. Also, thinning the chain is needed to avoid biased estimation of correlated samples and reduce processing and storing costs. Thinning is done by not considering the correlated samples and averaging over every t -th iteration Carlo [2004]. The details of the following equations can be found in "Proposed Method Details," Section 2 of the supplementary document for this paper sup [2022].

Sampling \mathbf{Y} : Using the *vec* operator, the posterior of \mathbf{Y} is a Gaussian distribution multiply unit step function, where the covariance $\Sigma_{\mathbf{Y}}$ and mean $\mu_{\mathbf{Y}}$ are given by:

$$\begin{aligned}
 \Sigma_{\mathbf{Y}} &= [((\mathbf{I}_M \otimes \mathbf{X}) \circ (\sigma_C^{-2} \mathbf{1}_{MN} \otimes \text{vec}(\mathbf{\Pi})))(\mathbf{I}_M \otimes \mathbf{X}^T) + (\mathbf{I}_D \otimes \mathbf{W}_Y^{-1})]^{-1} \\
 \mu_{\mathbf{Y}} &= \Sigma_{\mathbf{Y}}((\mathbf{I}_M \otimes \mathbf{X}) \circ (\sigma_C^{-2} \mathbf{1}_{MN} \otimes \text{vec}(\mathbf{\Pi})) \text{vec}(\mathbf{C}))
 \end{aligned} \tag{5}$$

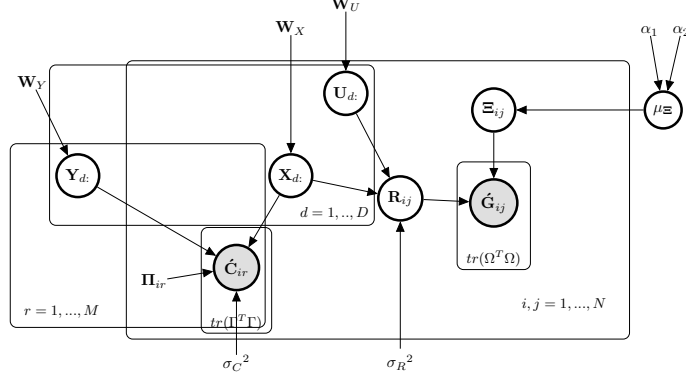


Figure 4: The generative Bayesian probabilistic representation of the proposed model (DiffStru).

When the covariance matrix is identity, for each cascade j , we can sample latent factor from a D -dimensional normal distribution multiply unit step function where the covariance matrix and the mean vector are given by:

$$\begin{aligned} \Sigma_{\mathbf{Y}}^{(j)} &= [\sigma_c^{-2}(\mathbf{X} \circ \Pi_{:,j})\mathbf{X}^T + \mathbf{I}_D]^{-1} \\ \mu_{\mathbf{Y}}^{(j)} &= \sigma_c^{-2}\Sigma_{\mathbf{Y}}^{(j)}(\mathbf{X} \circ \Pi_{:,j})\mathbf{C}_{:,j} \end{aligned} \quad (6)$$

Sampling Ξ : As discussed in the previous section, $\Xi_{ij} = 1$ when $\Gamma_{ij} = 1$, and hence the conditional posterior density of Ξ is:

$$P(\Xi_{ij} | \mathbf{G}_{ij} = 0, -) = [\Xi_{ij}(1 - f(\mathbf{R}_{ij})) + (1 - \Xi_{ij})\mathbb{I}(\mathbf{G}_{ij} = 0)] \times \mu_{\Xi}^{\Xi_{ij}}(1 - \mu_{\Xi})^{1 - \Xi_{ij}} \quad (7)$$

But this value should be inferred for elements when $\Gamma_{ij} = 0$. In this case $P(\Xi_{ij})$ is a Bernoulli distribution:

$$\begin{aligned} P(\Xi_{ij} = 0 | \mathbf{G}_{ij} = 0, -) &\propto (1 - \mu_{\Xi}) \\ P(\Xi_{ij} = 1 | \mathbf{G}_{ij} = 0, -) &\propto \mu_{\Xi}(1 - f(\mathbf{R}_{ij})) \end{aligned} \quad (8)$$

Therefore, the sampling posterior is:

$$\begin{aligned} P(\Xi_{ij} = 1 | \mathbf{G}_{ij} = 1, -) &= 1 \\ P(\Xi_{ij} | \mathbf{G}_{ij} = 0, -) &= \text{Ber}(\xi) \quad \xi = \frac{\mu_{\Xi} - \mu_{\Xi}f(\mathbf{R}_{ij})}{1 - \mu_{\Xi}f(\mathbf{R}_{ij})} \end{aligned} \quad (9)$$

Sampling μ_{Ξ} : Due to the use of conjugate prior for μ_{Ξ} , their conditional distribution will be a Beta distribution. Equation (10) shows the details for μ_{Ξ} :

$$P(\mu_{\Xi} | -) \sim \text{Beta}(\mu_{\Xi} | \alpha_1 + \sum_{i,j} \Xi_{ij}, \alpha_2 + N^2 - \sum_{i,j} \Xi_{ij}) \quad (10)$$

Sampling \mathbf{U} : Given the other latent variables, the posterior of \mathbf{U} is, we can sample $\text{vec}(\mathbf{U})$ from the normal distribution, where the covariance $\Sigma_{\mathbf{U}}$ and mean $\mu_{\mathbf{U}}$ are given by:

$$\begin{aligned} \Sigma_{\mathbf{U}} &= [((\sigma_R^{-2}\mathbf{I}_N) \otimes (\mathbf{X}\mathbf{X}^T)) + (\mathbf{I}_D \otimes \mathbf{W}_U^{-1})]^{-1} \\ \mu_{\mathbf{U}} &= \Sigma_{\mathbf{U}}[(\sigma_R^{-2}\mathbf{I}_N \otimes \mathbf{X})\text{vec}(\mathbf{R})] \end{aligned} \quad (11)$$

With the identity covariance matrix, for each user i , we can sample latent factor from a D -dimensional normal distribution with the following mean and covariance.

$$\Sigma_{\mathbf{U}} = [\sigma_r^{-2}\mathbf{X}\mathbf{X}^T + \mathbf{I}_D]^{-1}; \quad \mu_{\mathbf{U}}^{(i)} = \sigma_r^{-2}\Sigma_{\mathbf{U}}\mathbf{X}\mathbf{R}_{:,i} \quad (12)$$

There is a problem in sampling the remaining variables of the joint distribution (4) because of the logistic likelihood function, which is not conjugate with other Gaussian terms. Hence, we utilize the Polya-Gamma latent variables Polson et al. [2013] by adding an auxiliary random variable Λ_{ij} (Fig. (5)) for approximating the logistic likelihood with a Gaussian distribution that can easily multiply with prior normal distributions.

$$\begin{aligned} P(\mathbf{G}_{ij} | \mathbf{R}_{ij}, \mathbf{E}_{ij} = 1) &= f(\mathbf{R}_{ij}) = \frac{1}{1 + e^{(-\mathbf{R}_{ij})}} = \frac{e^{(\mathbf{R}_{ij})}}{e^{(\mathbf{R}_{ij})} + 1} \\ &= \frac{1}{2}e^{(\mathbf{G}_{ij} - \frac{1}{2})\mathbf{R}_{ij}} \int_0^{\infty} e^{-\frac{\Lambda_{ij}\mathbf{R}_{ij}^2}{2}} P(\Lambda_{ij})d\Lambda_{ij} \end{aligned} \quad (13)$$

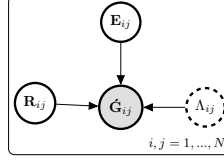


Figure 5: Adding Polya-gamma auxiliary variables (Λ_{ij}) for presenting the model as conditionally conjugate.

where, $P(\Lambda_{ij}) \sim PG(\Lambda_{ij}|1, 0)$. By conditioning (13) on auxiliary variable, we obtain:

$$P(\mathbf{G}_{ij}|\mathbf{R}_{ij}, \mathbf{E}_{ij} = 1, \Lambda_{ij}) \propto \exp((\mathbf{G}_{ij} - 0.5)\mathbf{R}_{ij} - \frac{1}{2}\Lambda_{ij}\mathbf{R}_{ij}^2) \quad (14)$$

Sampling Λ : The sampling of Λ is given by:

$$P(\Lambda_{ij}|-) \propto P(\mathbf{G}_{ij}|\mathbf{R}_{ij}, \mathbf{E}_{ij} = 1, \Lambda_{ij})P(\Lambda_{ij}) \sim PG(\Lambda_{ij}|1, \mathbf{R}_{ij}) \quad (15)$$

Sampling \mathbf{X} : The posterior distribution of $\text{vec}(\mathbf{X}^T)$ is a normal distribution with following covariance and mean:

$$\begin{aligned} \Sigma_{\mathbf{X}} &= [((\mathbf{Y} \otimes \mathbf{I}_N) \circ (\sigma_c^{-2}(\text{vec}(\mathbf{\Pi}))^T))(\mathbf{Y}^T \otimes \mathbf{I}_N)] + [\sigma_R^{-2}(\mathbf{U} \otimes \mathbf{I}_N)(\mathbf{U}^T \otimes \mathbf{I}_N)] + (\mathbf{I}_D \otimes \mathbf{W}_X^{-1})^{-1} \\ \mu_{\mathbf{X}}^T &= \Sigma_{\mathbf{X}} [((\mathbf{Y} \otimes \mathbf{I}_N) \circ (\sigma_c^{-2}(\text{vec}(\mathbf{\Pi}))^T))\text{vec}(\mathbf{C}) + (\sigma_R^{-2}(\mathbf{U} \otimes \mathbf{I}_N)\text{vec}(\mathbf{R}))] \end{aligned} \quad (16)$$

Assuming an initialized identity covariance, for each user i , \mathbf{X} can be sampled from a D -dimensional normal distribution with following parameters:

$$\begin{aligned} \Sigma_{\mathbf{X}}^{(i)} &= [\sigma_c^{-2}(\mathbf{Y} \circ \mathbf{\Pi}_{i:})\mathbf{Y}^T + \sigma_r^{-2}\mathbf{U}\mathbf{U}^T + \mathbf{I}_D]^{-1} \\ \mu_{\mathbf{X}}^{(i)} &= \Sigma_{\mathbf{X}}^{(i)} [\sigma_c^{-2}(\mathbf{Y} \circ \mathbf{\Pi}_{i:})\mathbf{C}_{i:}^T + \sigma_r^{-2}\mathbf{U}\mathbf{R}_{i:}] \end{aligned} \quad (17)$$

Sampling \mathbf{R} : The sampling of \mathbf{R} is given by $\mathcal{N}(\mathbf{R}_{ij}|\mu_{R_{ij}}, 1)$, where the mean $\mu_{R_{ij}}$ is:

$$\mu_{R_{ij}} = \frac{\Xi_{ij}(\mathbf{G}_{ij} - 0.5)\sigma_R^2 + \mathbf{X}_{i:}^T\mathbf{U}_{:j}}{\Xi_{ij}\Lambda_{ij}\sigma_R^2 + 1} \quad (18)$$

5.3 Predicting Missing Data

By learning the latent matrices \mathbf{X} , \mathbf{Y} , \mathbf{U} , and ξ , $\hat{\mathbf{G}} = \sigma(X^T U)$ can be estimated. For the missing entry of $\hat{\mathbf{G}}_{ij}$, $\hat{\mathbf{G}}_{ij}$ is given by:

$$\hat{\mathbf{G}}_{ij} = \begin{cases} 0 & \text{if } ((\xi_{ij} = 0) \vee (\sigma(X_{i:}^T U_{:j}) \leq \delta_G)) \\ 1 & \text{else} \end{cases} \quad (19)$$

where δ_G is a threshold for distinguishing links and non-links. To approximate the missing values of $\hat{\mathbf{C}}_{ij}$, first we define the infection probability of the node i in the cascade j with \mathbf{P}_{ij} , and if $\mathbf{P}_{ij} \succ \delta_C$ then $\hat{\mathbf{C}}_{ij}$ is estimated by $X_{i:}^T Y_{:j}$ with mapping the negative and the out of interval $[0, T]$ values to uninfected state:

$$\begin{aligned} z &= X_{i:}^T Y_{:j}, \\ \hat{\mathbf{C}}_{ij} &= \begin{cases} 0 & \text{if } ((\mathbf{P}_{ij} \leq \delta_C) \vee (z < 0 \vee z > T)) \\ z & \text{else} \end{cases} \end{aligned} \quad (20)$$

The infection probability matrix is defined as $\mathbf{P} = \mathbf{\Pi}^T \mathbf{A}$, where $\mathbf{\Pi}$ is the mask diffusion matrix that we have already defined. \mathbf{A} is a $N \times N$ infection transfer matrix, that each of its (i, j) elements indicates the probability of infection propagation from node i to node j as Equation (21), where $|\{\ast\}|$ is the cardinality of set \ast . In other words, it represents the ratio of the number of cascades that node i has been involved in before node j , in comparison to the total number of cascades each of them participated in.

$$\mathbf{A}_{i \rightarrow j} = \frac{|\{(\hat{\mathbf{C}}_{i:} \cap \hat{\mathbf{C}}_{j:}) | (\hat{\mathbf{C}}_{i:} < \hat{\mathbf{C}}_{j:})\}}{|\{(\hat{\mathbf{C}}_{i:} \cup \hat{\mathbf{C}}_{j:})\}} \quad (21)$$

From the diffusion observations, we obtain the probability that the simultaneous concurrence of two nodes i and j in cascades is due to the infection transmission from i to j . The DiffStru algorithm is presented as Algorithm (2).

Algorithm 2: DiffStru Algorithm

Input : Observed Matrix Cascade $\hat{\mathbf{C}}$, Observed Matrix Graph $\hat{\mathbf{G}}, \alpha_1, \alpha_2, \sigma_C^2, \sigma_R^2$, max iteration T , burn in b , thinning k , and latent factor D

Output : Inferred Matrix Cascade $\hat{\mathbf{C}}$, Inferred Matrix Graph $\hat{\mathbf{G}}$

- 1 $(N, N) = \text{shape}(\mathbf{G});$
 - 2 $(N, M) = \text{shape}(\mathbf{C});$
 - 3 Initialize $\mathbf{W}_Y^{-1}, \mathbf{W}_X^{-1}, \mathbf{W}_U^{-1}$, with Equation (26) or identity matrix
 - 4 Initialize $\mathbf{X}^{D \times N}, \mathbf{R}^{N \times N}, \mathbf{Y}^{D \times M}, \mathbf{U}^{D \times N}, \mathbf{\Lambda}^{N \times N}, \mu^{N \times N}$ randomly Initialize binary mask $\Xi^{N \times N}$ and $\Pi^{N \times M}$ from $\hat{\mathbf{G}}$ and $\hat{\mathbf{C}}$;
 - 5 **for** $t=1, \dots, T$ **do**
 - 6 Sample \mathbf{R}^t from normal with (18)
 - 7 Sample each element of Ξ_{ij}^t from (9)
 - 8 Sample \mathbf{X}^t from (16) or (17)
 - 9 Sample \mathbf{U}^t from (11) or (12)
 - 10 Sample \mathbf{Y}^t from (5) or (6)
 - 11 Sample each element of Λ_{ij}^t from (15)
 - 12 Sample μ^t from (10)
 - 13 **end**
 - 14 $\mathbf{X} = \frac{k}{T-b} \sum_{i=1}^{\frac{T-b}{k}} \mathbf{X}^{b+ki}, \mathbf{Y} = \frac{k}{T-b} \sum_{i=1}^{\frac{T-b}{k}} \mathbf{Y}^{b+ki}$
 - 15 $\mathbf{U} = \frac{k}{T-b} \sum_{i=1}^{\frac{T-b}{k}} \mathbf{U}^{b+ki}, \Xi = \frac{k}{T-b} \sum_{i=1}^{\frac{T-b}{k}} \Xi^{b+ki}$
 - 16 Compute $\hat{\mathbf{G}}$ from (19)
 - 17 Compute $\hat{\mathbf{C}}$ from (20)
-

5.4 Computational Complexity

The most time-consuming part of the algorithm is sampling three latent factors. In a parallel environment, the time complexity of sampling of variable \mathbf{U} as Equation (12) is $O(D^3 + D^2N)$, variable \mathbf{X} based on Equation (17) is $O(D^3 + D^2N + D^2M)$, and variable \mathbf{Y} from Equation (6) is equal to $O(D^3 + D^2N)$. Hence, in T iterations, the total complexity of the algorithm is equal to $O(TD^2(D + N + M))$, which is linear with respect to N, M and $D \ll M, N$.

6 Numerical and Simulation Results

For supporting different network scales, we implement DiffStru in a distributed framework named Ray Moritz et al. [2018], which is an open-source framework for scaling up Python applications from single machines to large clusters. Depending on the amount of input data and resources required in each step of the algorithm’s iteration, new machines can enter the cluster during the run of the method. We also used Ray for tuning hyper-parameters of our method and the rest of the works with which we have compared. We ran all experiments on a server with an Intel® Core™ i9-7980XE Extreme Edition Processor equipped with 128GB of RAM and two NVIDIA GeForce GTX 1080 TI, running Ubuntu 18.04. Since no related work addresses joint completion of the missing parts of diffusion and structure, we separately compare DiffStru against different link prediction, network inference, and cascade correction and prediction methods.

Structure part competitors: We chose Adamic Adar (**AA**) Adamic and Adar [2003], Resource Allocation (**RA**) Ou et al. [2007], and Common Neighbor (**CN**) Lorrain and White [1971] as classical link prediction methods as well as the recent fusion matrix factorization method (**FPMF**) Wang et al. [2018]. The classical approaches calculate the similarity weight of any unlinked pairs of nodes. Unobserved links can be obtained by sorting the weights in ascending order and cutting the top pairs. FPMF is a matrix factorization method that fuses some asymmetric and symmetric topological metrics with an adjacent structure matrix to learn the latent factor of nodes with gradient methods. Link-Corrected Prediction Algorithm **LCPA** Chai et al. [2022] is a maximum likelihood method for estimating hidden links. These works are based on the incomplete structure of networks as inputs.

From the network inference category, we selected the **Netrate** Gomez-Rodriguez et al. [2013], **DANI** Ramezani et al.

[2017], and **REFINE** Kefato et al. [2019] methods that find hidden links using fully observed diffusion information. We used partially observed cascades as the input of these methods.

Cascade part competitors: There is no work for mining the omitted infected nodes in the diffusion category by estimating their infection time. To compare this part of DiffSru, we chose a cascade prediction technique called **DeepDiffuse** Islam et al. [2018]. DeepDiffuse tries to predict the next node in a cascade by ranking the possible candidates by estimating a single time. However, this method does not pay attention to missing data and aims to predict the next step of the cascade sequence by assuming that the observed steps are complete. Therefore, to compare DeepDiffuse with DiffSru, we should input the cascade sequence up to any missing step point to the model to obtain the prediction. Then we can compare the error of the predicted next infection time. As a baseline, we fit a polynomial regression model (with degrees one and two, named Reg-1 and Reg-2) on a sorted cascade sequence. Then for any missing node k , which is infected after node i and before node j , we find the related time from the learned regression model using the mean indexes of node i and j in the sequence. We provide more prior knowledge for both DeepDiffuse and baseline methods compared to DiffSru. Both methods know the position of two nodes in a cascade where the missing has happened. Therefore, computing the missed infection time is approximated relative to the time of the previous node. However, DiffSru does not utilize this information. While DeepDiffuse predicts the next infected node with its infection time, other cascade prediction methods included in Section (3) do not predict time. Since we aim to detect missing nodes with their infection time, DeepDiffuse is the only comparison candidate from the "cascade correction and prediction" category. For more experiments, we used **NetFill** Sundareisan et al. [2015], which finds the missing nodes in a cascade without their infection time by using the entire structure of the network. The only way to compare DiffSru and NetFill is based on the inferred number of missed infection nodes.

Joint Weighted Nonnegative Matrix Factorization (**JWNMF**) Tang [2023] is another link prediction method using non-negative matrix factorization and binary attributes of nodes. By defining the cascade participle as a node attribute, we construct this attribute matrix from partially observed cascades. Whenever a node is infected in a cascade, its related attribute is 1, otherwise 0. By doing this, we make **JWNMF** the closest related work with the same inputs as DiffSru.

Our experiments were conducted using the official code provided by the authors of all related works, except REFINE and JWNMF (REFINE and JWNMF codes were not available). We implemented their methods ourselves based on the explanations provided in their papers. We used ray hyper-parameter tuning for each of these two methods to achieve the best results. Our implementations of REFINE¹ and JWNMF² are available on GitHub.

6.1 Description of the Datasets

Synthetic: We generated synthetic directed graphs resembling real social networks independent of the proposed model. The LFR (Lancichinetti-Fortunato-Radicchi) network is a benchmark having interesting real-world features such as community structure and power-law degree distribution Lancichinetti et al. [2008]. We generated three different artificial LFR networks having 50, 100, and 400 nodes with parameters: mixing parameter 0.1, degree sequence exponent 2, community size distribution exponent 1, and zero number of overlapping nodes. Then, we simulated different independent cascades on each graph using the method described in Gomez-Rodriguez et al. [2012]. The transmission model was exponentially distributed with parameters: $\alpha=1$, a mixture of exponential=1, and $\beta=0.5$.

Real world: As stated earlier, data loss in real-world datasets is unavoidable. Thus, creating a test scenario on these datasets will cause an extreme lack of information, and no proper ground truth exists for evaluation. Therefore, we consider a dense part of these networks (by choosing a big community) with a density of about 0.1 to test and perform data deletion scenarios. Therefore, we applied this approach to two real datasets: A Twitter dataset during October 2010 with a network of 6642 links between followers and time sequence of retweeting between 2144 activity of users Hodas and Lerman [2014]. Also, a Memestracker dataset with 4828 memes propagation between websites during April 2009 with a 41404 graph connection Leskovec et al. [2009].

6.2 Evaluation Metrics

To evaluate the results of DiffSru, we compared its performance from structural and diffusion points of view. The observed \hat{G} and \hat{C} are the training sets, and we treat them as known data, while the missing parts of $G \setminus \hat{G}$ and $C \setminus \hat{C}$ are testing sets, and no knowledge about these sets is used in learning our model. If the output of models is represented with \hat{G} and \hat{C} , then we evaluate the reconstruction of estimated matrices and accuracy of different aspects with the following metrics:

SRE: With Signal Reconstruction Error (SRE) Iordache et al. [2011], we can evaluate the success rate in reconstructing the ground-truth matrix - the higher this metric, the lower the recovery noise ratio to the original

¹<https://github.com/AryanAhadnia/REFINE>

²<https://github.com/AryanAhadnia/JWNMF>

matrix. For the ground-truth matrix \mathbf{Z} , if the estimated matrix is $\hat{\mathbf{Z}}$, SRE metric is approximated as Iordache et al. [2011]:

$$SRE = \frac{\|\mathbf{Z}\|_2^2}{\|\hat{\mathbf{Z}} - \mathbf{Z}\|_2^2} \quad (22)$$

AUC: Since we face an unbiased binary classification in reconstructing the structural information (matrix \mathbf{G}), the area under the receiver operating characteristic curve is a useful metric for evaluation, which is independent of the threshold setting. AUC measures the probability of randomly selecting linked and unlinked pairs of nodes and checking if the probability of linked pairs is higher than unlinked pairs. The higher AUC value indicates the better performance of the model in classifying the two classes.

$$AUC = \frac{\sum_{(a,b),(c,d) \in (\mathbf{G} \setminus \hat{\mathbf{G}})} [\mathbb{I}(\hat{\mathbf{G}}(a,b) > \hat{\mathbf{G}}(c,d)) + 0.5(\hat{\mathbf{G}}(a,b) = \hat{\mathbf{G}}(c,d))] \times \mathbb{I}(\mathbf{G}(a,b) = 1, \mathbf{G}(c,d) = 0)}{\sum_{(a,b),(c,d) \in (\mathbf{G} \setminus \hat{\mathbf{G}})} \mathbb{I}(\mathbf{G}(a,b) = 1, \mathbf{G}(c,d) = 0)} \quad (23)$$

Precision, Recall, and F-measure: By applying a threshold on probabilities of matrix $\hat{\mathbf{G}}$, we can map the elements to zero and one values. The precision and recall are defined below, and F-measure is the weighted harmonic mean of recall and precision.

$$Precision = \frac{\hat{\mathbf{G}} = 0 \wedge \mathbf{G} = 1 \wedge \hat{\mathbf{G}} = 1}{\hat{\mathbf{G}} = 1 \wedge \hat{\mathbf{G}} = 0}, Recall = \frac{\hat{\mathbf{G}} = 0 \wedge \mathbf{G} = 1 \wedge \hat{\mathbf{G}} = 1}{\mathbf{G} = 1 \wedge \hat{\mathbf{G}} = 0} \quad (24)$$

Accuracy: Is a metric for measuring the portion of correctly classified pairs:

$$ACC = \frac{(\hat{\mathbf{G}} = 0 \wedge \mathbf{G} = 1 \wedge \hat{\mathbf{G}} = 1) + (\mathbf{G} = 0 \wedge \hat{\mathbf{G}} = 0)}{\hat{\mathbf{G}} = 0} \quad (25)$$

MCC: The Matthews Correlation Coefficient metric Matthews [1975] is suitable for measuring the quality of binary ill-balanced classification, which utilizes the ratios of true positives, true negatives, false positives, and false negatives. When the value of this metric is near 1, the estimated value is closer to reality, while the value closer to 0 shows the estimator prediction is close to random, and the -1 value indicates a complete disagreement.

MAP@K: The Mean Average Precision is utilized for measuring the performance of DeepDiffuse Islam et al. [2018]. If we have $\#A$ number of missing activities, the ground truth of these test samples has one value, while DeepDiffuse outputs an ordered list of nodes. MAP@K means averaging overall prediction of $\#A$ samples based on the @K top

first of the algorithm output list $\frac{\sum_{i=1}^{\#A} [\mathbb{I}(r_i \leq K) (\frac{1}{r_i})]}{\#A}$

RMSE: We measure the Root Mean Square Error (RSME) between \mathbf{C} and $\hat{\mathbf{C}}$ for the timestamp of observed training data and test unobserved nodes. There is no fixed threshold limit for RMSE, and the lower value indicates a better fit.

6.3 Experiments Setting

The first step toward setting inputs of experiments is simulating the missing information in all datasets. Missing data can occur at random events, which leads to an unbiased analysis. However, in some real cases, data missing may happen because of sampling techniques or some limitations of APIs that are not random. For example, we cannot gather all the connections of a high-degree node that directs us to the missing data. Since we do not have any assumption about deletion in the proposed method, we ran different experiments for two types of missing data.

Random missing: We eliminate data with uniform distributions to simulate random missingness. For this purpose, we first choose a remove rate $\theta \in [0, 1]$. Then for each link of structure or activity in the diffusion, a random value τ is generated from a uniform distribution on $[0, 1]$, and if $(\tau < \theta)$, we remove that data.

Non-random missing: For a non-random scenario, we randomly remove the links between nodes whose outdegree is higher than five. Besides, we calculate the activities of each node, and activity removal is done randomly over the set of nodes with more than five participants. By default, runs were over 1000 iterations with burn-in of 900 and thinning of 1. If there is a change in the setting of any scenario, we have listed the new settings.

6.4 Hyper-parameters Setting

The link prediction between any two nodes is correlated with the structural properties of nodes so that the more similar structural relations of two nodes will lead to more likelihood of a link between them. Furthermore, the cascades that have infected more similar nodes are more alike in their diffusion path. Suppose that Θ_{ij}^X is a measure of the structural similarity between two nodes i and j in a network, then the larger value of Θ_{ij}^X indicates the lower distance between

$\mathbf{X}_{:i}$ and $\mathbf{X}_{:j}$. Therefore, for any pair of nodes, we look for the minimal value of the following equation:

$$\sum_{i=1}^N \sum_{j=1}^N \Theta_{ij}^X \|\mathbf{X}_{:i} - \mathbf{X}_{:j}\|_2^2 = \sum_{i=1}^N \sum_{j=1}^N \sum_{d=1}^D (\Theta_{ij}^X \mathbf{x}_{di}^2 - \Theta_{ij}^X \mathbf{x}_{di} \mathbf{x}_{dj}) = \sum_{d=1}^D \mathbf{x}_d^T (\zeta^X - \Theta^X) \mathbf{x}_d. \quad (26)$$

where $\mathcal{L}^X = (\zeta^X - \Theta^X)$ is a Laplacian matrix with $\zeta_{ii}^X = \sum_{j=1}^N \Theta_{ji}^X$ is a diagonal matrix. This property of \mathbf{X} is

equivalent to multivariate Gaussian distribution with zero mean and inverse covariance matrix $\mathbf{W}_X^{-1} = \mathcal{L}^X$. Similarly, we can model \mathbf{U} and \mathbf{Y} . To initialize the covariance matrix of hyper-parameters, we can set it to an identity matrix without modeling the correlation of nodes and cascades (independent priors) or considering the relation of these components (correlated priors). For dependent priors, we use the similarity of nodes as the number of common neighbors in the partially observed structure network for Θ^X and Θ^U . In contrast, the similarity of cascades is defined by the ij entry of Θ^Y , which is the number of common nodes in i -th and j -th cascades. Other hyper-parameters are set as, in Equation (20) where $\delta_G = 0.5$ and δ_C in Equation (19) is set as the mean value of all \mathbf{P} elements. Moreover, $\sigma_C^2 = 1$, $\sigma_R^2 = 1$, $D = 8$, $\alpha_1 = 0.2$, and $\alpha_2 = 0.3$. All the elements of matrix \mathbf{X} , \mathbf{U} , and \mathbf{Y} have been initialized by sampling from the Rectified Normal Distribution so that all elements are positive.

6.5 Model Analysis

In this section, we verify the impact of different parameters on the performance of DiffStru and focus on its ability to solve problems in various situations. Some experiments on synthetic LFR networks are intended to answer the following questions:

(1) What is the best size of the latent space (hyper-parameter D)?

Learning the latent factors of the model in the smaller dimension will reduce the complexity of inference calculations. On the other hand, the model focuses on completing the structure and diffusion matrices simultaneously. While the measurement metrics for completing these matrices differ, we scan for a lower dimension where the best results can be achieved in both structure and diffusion spaces. Because of random initialization, we ran the model multiple times and reported the mean and standard deviation of metrics, as shown in Fig. (6). Here, the different values of latent factors are analyzed, and $D = 8$ is the best choice with a higher mean value and lower standard deviation in terms of AUC, precision, and F-measure for mining missing links, as well as lower mean and standard deviation for RMSE in finding missing activities.

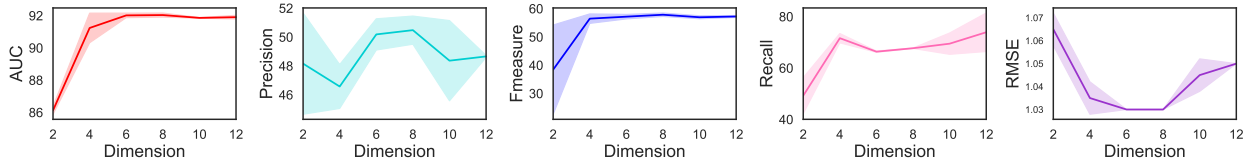


Figure 6: Comparing structural and diffusion metrics against different values of latent space in the LFR100 dataset.

(2) How does the density of the ground-truth network structure affects the inference of missing information?

We simulated four different LFR datasets with 50 nodes and 50 generated cascades with different mixing parameters to have various densities. Then in each dataset, we randomly removed the activities in cascades with 0.3 rates and the remaining 60% of links as observed data. The results are reported based on an average of five training sets and their standard deviations. The sampling set had 2000 iterations, burn-in of 1500, and thinning of 5. Fig. (7a) shows the ground-truth graph’s structural metrics against different densities. As illustrated, increasing the amount of information improves the method’s performance. As shown in Fig. (7b), more links lead to better cascade estimation. Moreover, we achieve acceptable results only by observing approximately half of the data in structure and diffusion layers.

(3) How is the performance of DiffStru even if there is no activity observation for a subset of users (e.g., users with private accounts)?

In the LFR50 dataset, we used the same removal setting as the previous analysis mentioned in question (2). We increased the amount of data deletion by removing the complete information of five rows of diffusion matrix to simulate the private user profiles. In addition to accessing half of the user’s activities, we did not have any data about the activities of five network nodes. Then, two settings of the proposed method (correlated and independent priors) were tested. Fig. (8) demonstrates the result of DiffStru when the hyper-parameter covariance matrix of the prior distribution is initialized with correlated side information and when the priors are independent by utilizing an identity matrix. We found that the dependent prior can increase the performance of DiffStru for both structure and diffusion information, especially when there are empty rows in the cascade matrix.

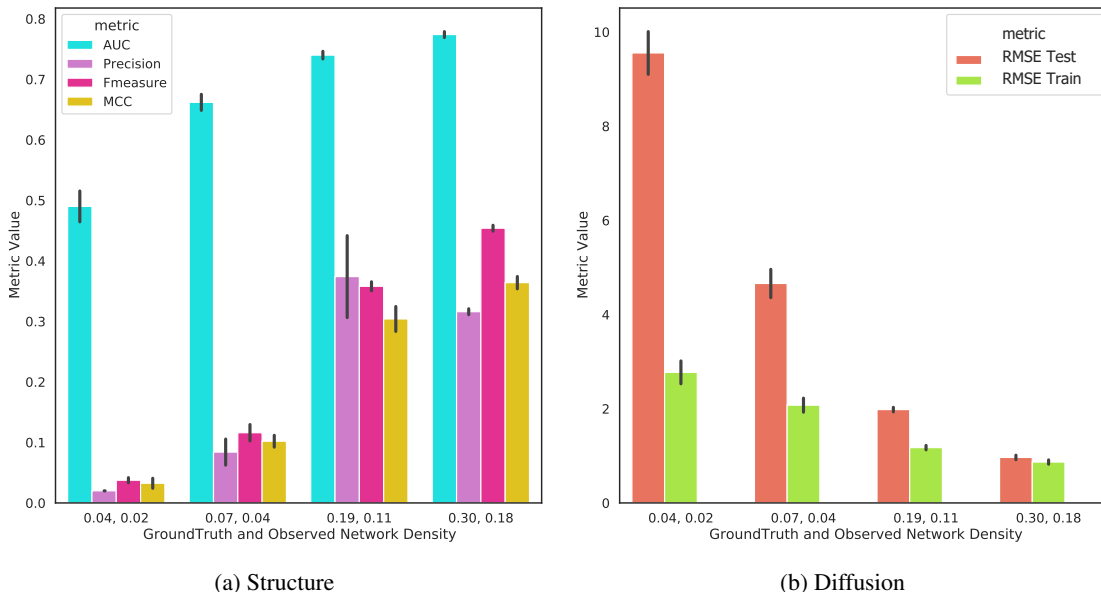


Figure 7: Impact of structure network density on LFR100 dataset. The horizontal axis of the plot represents the density of the ground truth and observed network. The input to the models is the observed network, which is less dense due to partially observed data (only 60% of links are observed).

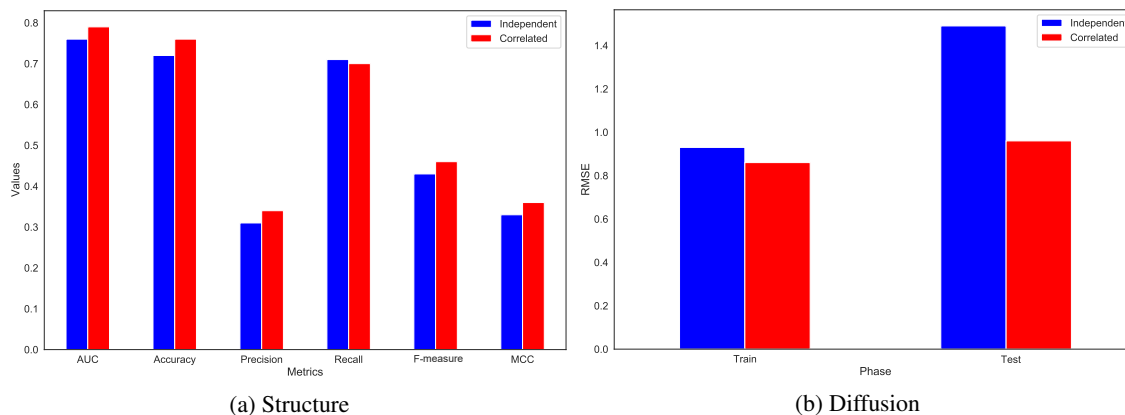


Figure 8: Effect of using correlated values for initializing the covariance matrix of prior distributions in LFR50 dataset.

(4) Can the learned latent factors be used for classification problems?

Each node and cascade can be represented with an embedded $D \times 1$ vector. LFR100 and LFR400 datasets have four and six ground-truth embedded community structures, respectively. We visualized the network nodes from the learned matrix \mathbf{X} and \mathbf{U} with the color of their communities as shown in Fig. (9a), (9b), (9d), and (9e), by using the PCA and t-SNE methods Maaten and Hinton [2008]. The figure illustrates that nodes' embedded learned features are separated in space according to their community labels. At the same time, we did not consider any assumptions about the community structure in DiffStru. Despite node classification, we do not have any ground truth for comparing the cascade classifications. Still, their embedded vectors based on the learned matrix \mathbf{Y} are shown in Fig. (9c) and (9f).

(5) What is the impact of the removal rate on the performance of DiffStru?

We investigated this issue on the LFR100 dataset. First, keeping the complete diffusion information, we examined the effect of link removal on the output of link mining. In this scenario, there was no test for cascades. The infection times estimator was tested in the training set of cascades. We randomly chose 203 samples of links from the structure network for the test. Then in experiments, we decreased the number of observations to find out the impact of link observation on the method's performance, as shown in Fig. (10). Second, we tested the different missing rates in the cascade data using the full observed graph of nodes. We chose 1655 activities as a test and did the experiments on various observations.

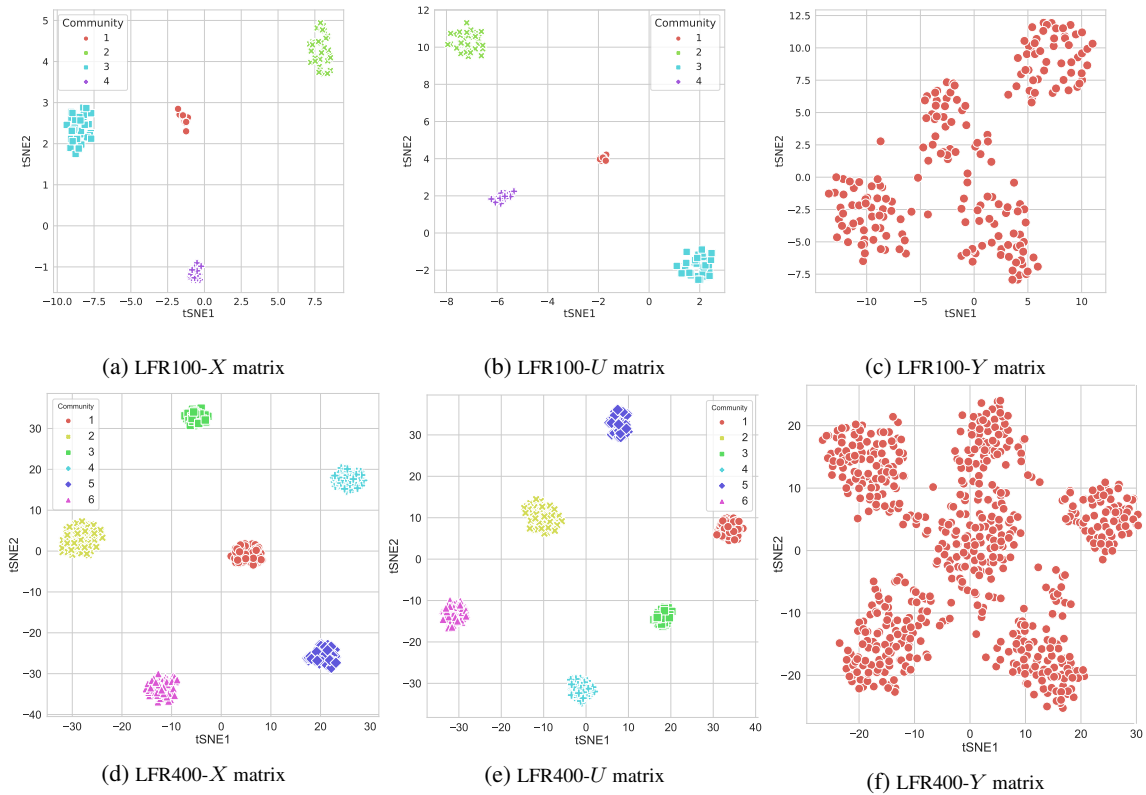


Figure 9: Visualization of learned latent feature matrices.

Here, we evaluated cascade information, and there were no missing links for testing. In Fig. (11), the performance of DiffStru on the two data splits is represented. RMSE on the training data is almost constant while decreasing by increasing the number of observations in the test set.

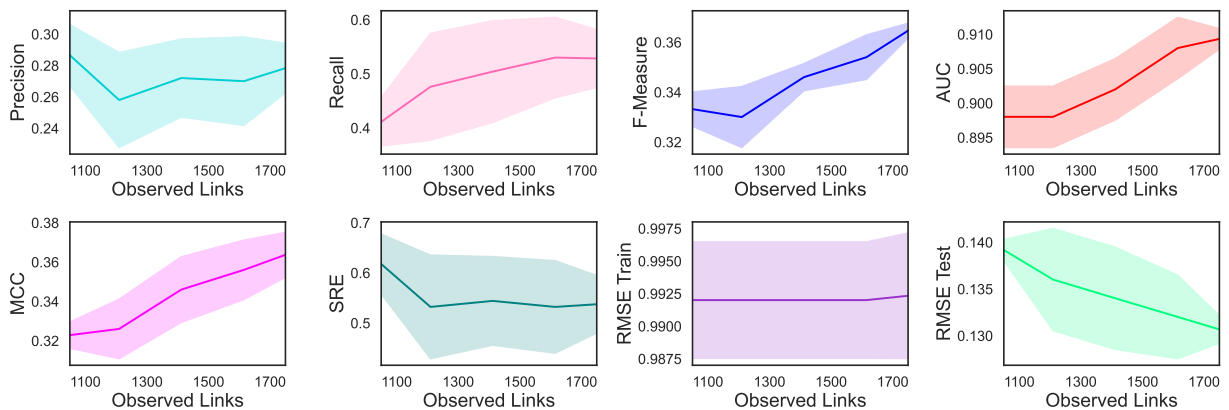


Figure 10: Impact of link removal rate on the link inferring and diffusion matrix results for LFR100 dataset.

6.6 Comparison

We tested DiffStru against related works on two synthetics and two real datasets. Based on the description in Section (6.3), different missingness patterns were utilized for generating the test scenarios. The Gibbs sampler of DiffStru was

Table 3: Comparison results for mining omitted activities of cascades in random and nonrandom deletion.

	Dataset	Metric	DiffStru	DeepDiff	Reg-1	Reg-2
Random	LFR100	RMSE	0.97	0.22	0.47	0.47
		MAP@10,50,100	-	7.90, 10.20, 10.60	×	×
	LFR400	RMSE	0.47	0.05	0.26	0.24
		MAP@10,50,100	-	1.11, 1.60, 1.90	×	×
	Twitter	RMSE	0.11	0.18	0.16	0.16
		MAP@10,50,100	-	12.70, 15.30, 15.40	×	×
Mem	RMSE	1.79	1.99	1.98	2.55	
	MAP@10,50,100	-	8.30, 10.04, 10.70	×	×	
Non-random	LFR100	RMSE	0.98	0.13	0.45	0.39
		MAP@10,50,100	-	11.10, 13.20, 13.50	×	×
	LFR400	RMSE	0.49	0.03	0.26	0.23
		MAP@10,50,100	-	1.30, 1.80, 2.00	×	×
	Twitter	RMSE	0.10	0.07	0.06	0.08
		MAP@10,50,100	-	5.70, 6.80, 7.30	×	×
Mem	RMSE	3.40	2.66	2.41	2.97	
	MAP@10,50,100	-	10.20, 12.00, 12.30	×	×	

run with 5000 iterations, burn-in of 4500, and thinning of 5. The comparison over the structural network is reflected in Table (4) for non-random and random missing.. In both cases, DiffStru outperforms others in different metrics, especially simultaneously in AUC and F-measure, which are essential performance metrics for imbalanced datasets. The input for CN, FPMF, AA, RA, and LCPA is the observed network, while Netrate, DANI, and REFINE use the observed cascades. DiffStru and JWNMF utilize both observed networks and cascades.

Analysis from the diffusion perspective is reported in Table (3). Notably, the range of RMSE value does not have a limited ceiling. The remarkable point is that DiffStru infers any missing cascade node with its infection time. Still, DeepDiffuse outputs a unique infection time and sorts all network nodes according to the probability suggested for the next infected node in the cascade sequence. While DiffStru exactly infers the missing node and its timestamp, one should evaluate the precision of DeepDiffuse for discovering the node. Besides, the output of DiffStru is a single node with a real-value time, while DeepDiffuse ranks the nodes. We also had to report the MAP@K metric for DeepDiffuse, while this metric is not necessary for DiffStru.

For the structural network, the ratio of unlinked pairs against the linked nodes is too high; hence, we face the problem of imbalanced data. AUC and F-measure are the popular metrics for comparing the imbalanced classification. In all cases of random and non-random missing in four different synthetic and real datasets, DiffStru outperforms the other methods in terms of AUC. AUC shows that the overall performance of DiffStru at all different thresholds is almost high. For real-world data, to have better interpretability, we should compare methods in terms of F-measure by choosing the best threshold for each classifier to explicitly assign samples to two different classes. DiffStru is better than all the competing methods in terms of F-measure, except for the Twitter dataset, in which the CN method has a slightly better F-measure. The same pattern occurs in the accuracy metric. However, accuracy is not a good metric for imbalanced applications. Moreover, the higher SRE values indicate that the oracle adjacency matrix is recovered with less error. On average, the performance of DiffStru is high for the SRE criteria. For the MCC metric, the probabilistic methods (first DiffStru, and then FPMF) have the best performance compared to the classical methods. Finally, the precision-recall curve for the competing methods is shown in Fig. (12). The break-even points of DiffStru are near 0.54,0.53,0.94, and

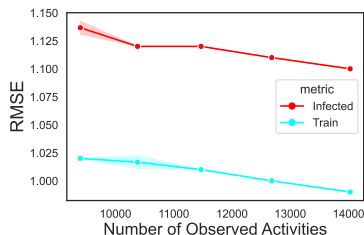


Figure 11: Impact of cascade removal rate on the infection time of diffusion matrix results for LFR100 dataset.

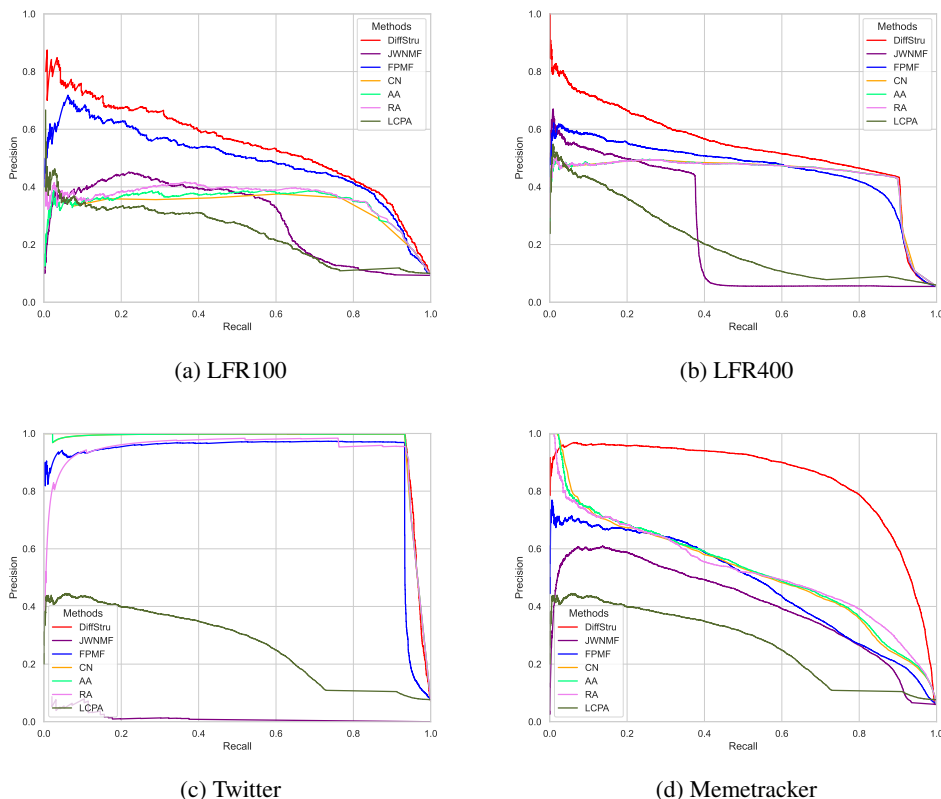


Figure 12: Precision-Recall curve on four different datasets. DiffStru achieves more break-even point value than other methods in completing the structural network.

0.79 for LFR100, LFR400, Twitter, and Memetracker datasets, respectively, which are all higher than the other methods. In general, DiffStru performs better than the competing methods regarding different metrics of Section (6.2). Based on the results, REFINE from the network inference category performed less well than other works because it is more sensitive to missing data, a factor it does not consider.

For the diffusion network comparisons, due to the lack of similar work, we had to make unfair comparisons with DeepDiffuse and Regression models for evaluating the RMSE of missing infection times. DeepDiffuse provides a sorted list of nodes instead of suggesting a specific missed node. The RMSE of infection times for the test data and MAP@K for predicting the name of a node are listed in Table (3). Since the regression models cannot detect the node’s identity, the corresponding table cells for MAP@K are filled with \times , and just RMSE is reported for its two versions, Reg-1 and Reg-2. On the other hand, DiffStru finds the missing node with its infection time, and its RSME is reported in the table. Because of the exact inference of DiffStru, its MAP@K is always 100%, and hence we have reported this fact by filling the corresponding cells in the table with $-$. It can be seen that despite the accurate identification of the missing node with DiffStru, its RMSE for infection time is in the appropriate range. In the RMSE comparison, it is important to note that the maximum value of RMSE is not limited to one. Fig. (13) illustrates the comparison between our proposed method, NetFill, and JWNMF. The JWNMF and NetFill algorithms attempt to determine the list of missing nodes without inferring the time of infection. Due to the incompleteness of the network structure, NetFill and JWNMF perform worse than DiffStru. A total number of 636 cascades participating nodes are missed in Twitter, while Diffstru detects 539, NetFill detects 9, and JWNMF detects 835. Among the 2954 cascades participating nodes missing for LFR100, DiffStru, NetFill, and JWNMF inferred 2202, 705, and 7934.

Table 4: Link prediction result for random and non-random deletion.

Dataset	Method	Non-random Missing					Random Missing				
		ACC	F1	AUC	MCC	SRE	ACC	F1	AUC	MCC	SRE
LFR100	DiffStru	67.85	56.35	91.58	0.52	0.95	90.54	57.68	91.64	0.54	0.98
	JWNMF	87.46	44.37	73.81	0.38	0.86	87.25	44.08	72.84	0.37	0.85
	FPMF	89.18	54.84	89.46	0.50	0.86	89.17	55.65	90.23	0.51	0.86
	CN	85.42	49.35	86.10	0.46	0.64	85.29	49.22	86.77	0.45	0.63
	AA	85.15	50.08	86.74	0.47	0.62	86.85	49.89	87.53	0.45	0.71
	RA	85.90	49.80	86.96	0.46	0.65	86.98	50.11	87.87	0.46	0.71
	LCPA	81.32	32.60	67.02	0.24	0.74	79.37	32.02	66.44	0.23	0.70
	Netrate	89.98	56.83	76.26	0.51	1.12	84.54	39.30	67.03	0.31	0.73
	DANI	81.03	42.37	86.16	0.38	0.70	82.57	43.42	86.65	0.39	0.73
	REFINE	85.51	44.86	83.98	0.39	0.80	86.29	47.24	80.63	0.42	0.82
LFR400	DiffStru	93.65	58.85	92.15	0.59	0.86	93.58	58.94	92.41	0.59	0.85
	JWNMF	93.67	39.07	59.54	0.35	0.92	94.01	40.51	58.38	0.37	0.95
	FPMF	93.55	57.99	92.08	0.57	0.86	93.33	55.44	91.86	0.54	0.82
	CN	93.08	58.38	91.91	0.59	0.79	93.08	58.39	92.14	0.59	0.79
	AA	93.09	58.38	91.94	0.59	0.79	93.10	58.39	92.16	0.59	0.79
	RA	93.09	58.40	91.94	0.59	0.79	93.09	58.40	92.15	0.59	0.79
	LCPA	91.35	31.12	72.48	0.27	0.84	92.48	32.43	70.72	0.28	0.85
	Netrate	93.04	45.89	74.63	0.43	0.79	91.38	37.58	70.68	0.34	0.63
	DANI	92.71	51.80	91.42	0.50	0.86	92.99	52.10	91.73	0.50	0.88
	REFINE	92.64	48.14	90.29	0.45	0.86	93.85	41.88	59.97	0.38	0.94
Twitter	DiffStru	99.82	98.75	99.84	0.99	40.45	99.50	96.40	98.76	0.96	14.34
	JWNMF	99.98	3.77	56.09	0.00	0.96	99.97	9.01	68.50	0.06	0.68
	FPMF	99.63	97.48	98.79	0.97	19.93	99.29	95.00	96.52	0.94	10.19
	CN	99.84	98.90	99.48	0.98	45.93	99.50	96.43	97.30	0.96	14.49
	AA	99.84	98.88	99.49	0.98	45.93	99.50	96.43	97.30	0.96	14.49
	RA	99.39	96.78	99.39	0.96	15.94	99.21	94.48	97.20	0.94	9.16
	LCPA	99.96	8.72	61.13	0.09	0.64	99.97	14.11	63.76	0.15	0.79
	Netrate	7.27	13.62	50.00	0.00	0.08	96.95	36.92	72.67	0.36	0.62
	DANI	99.51	0.37	54.74	0.01	0.16	99.80	0.54	55.78	0.01	0.25
	REFINE	99.98	0.06	71.29	0.00	1.00	99.46	0.52	61.94	0.01	0.15
Memetracker	DiffStru	70.25	80.99	98.33	0.80	2.65	97.53	79.42	97.74	0.78	2.43
	JWNMF	92.51	48.91	87.59	0.45	0.89	92.55	47.73	86.97	0.44	0.89
	FPMF	93.43	51.85	92.18	0.48	0.97	94.04	51.21	91.08	0.48	0.95
	CN	93.27	55.19	94.58	0.53	0.88	91.00	54.03	93.33	0.51	0.92
	AA	93.17	55.75	94.81	0.53	0.88	90.99	54.50	93.52	0.52	0.90
	RA	94.08	58.03	95.46	0.55	1.00	91.56	54.72	93.95	0.52	0.91
	LCPA	88.38	36.69	73.89	0.31	0.81	87.47	36.46	74.16	0.31	0.78
	Netrate	96.24	54.40	68.68	0.60	1.60	95.68	43.84	64.04	0.52	1.39
	DANI	97.17	69.31	76.51	0.71	1.45	97.07	67.81	75.65	0.70	1.43
	REFINE	88.06	34.67	73.49	0.31	0.70	87.47	26.33	68.78	0.21	0.69

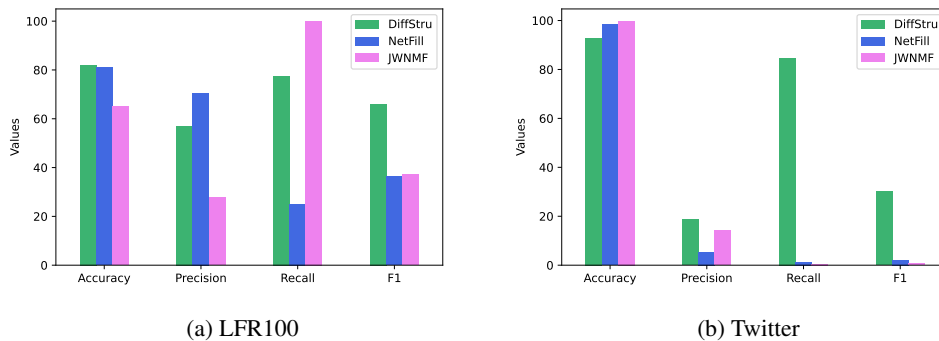


Figure 13: Detection of missing nodes in cascades without inferring the infection time.

7 Conclusion and Discussion

Although, in the past, researchers have worked on predicting the missing links of the network using existing links or inferring the structure from the cascades, completing cascades and links with the concurrent incompleteness in both of them has not been considered. In this paper, we presented a novel generative model called DiffStru by combining a network’s partially observed structure and diffusion information to infer the missing data efficiently. We embedded the observations in a low-dimensional latent space by fitting suitable distributions and estimating parameters with Gibbs sampling. DiffStru learns the latent factors during inference and can be utilized to solve other related network classification problems, such as community detection. We conducted several experiments on synthetic and real datasets to measure the effectiveness of DiffStru. To extend the proposed method, we can use different prior distributions for different link observer variables if we can obtain more network data, such as the profile and features of users. In future work, instead of the inner product of latent matrices, a deep-learning approach can be utilized for model inference to capture the complex relations of the data. In addition, our generative model can be extended to support more coupling relations. Another future direction of this work is extending the model to a dynamic framework by using the diffusion and structure of previous snapshots to forecast the next step of network evolution and predict the cascade sequences. Therefore, the model can infer the addition and removal of links caused by users joining or leaving the network. The creation time of links can also be estimated.

References

- Norases Vesdapunt and Hector Garcia-Molina. Identifying users in social networks with limited information. In *2015 IEEE 31st International Conference on Data Engineering*, pages 627–638, 2015.
- Václav Belák, Afra Mashhadi, Alessandra Sala, and Donn Morrison. Phantom cascades: The effect of hidden nodes on information diffusion. *Computer Communications*, 73:12 – 21, 2016.
- Eldar Sadikov, Montserrat Medina, Jure Leskovec, and Hector Garcia-Molina. Correcting for missing data in information cascades. In *Proceedings of the Fourth ACM International Conference on Web Search and Data Mining*, page 55–64. Association for Computing Machinery, 2011.
- Demetris Antoniadis and Constantine Dovrolis. Co-evolutionary dynamics in social networks: A case study of twitter. *Computational Social Networks*, 2(1):14, 2015.
- Mehrdad Farajtabar, Yichen Wang, Manuel Gomez-Rodriguez, Shuang Li, Hongyuan Zha, and Le Song. Coevolve: A joint point process model for information diffusion and network evolution. *The Journal of Machine Learning Research*, 18(1):1305–1353, 2017.
- Lilian Weng, Jacob Ratkiewicz, Nicola Perra, Bruno Gonçalves, Carlos Castillo, Francesco Bonchi, Rossano Schifanella, Filippo Menczer, and Alessandro Flammini. The role of information diffusion in the evolution of social networks. In *Proceedings of the 19th ACM SIGKDD international conference on Knowledge discovery and data mining*, pages 356–364, 2013.
- J. Zhang, Z. Fang, W. Chen, and J. Tang. Diffusion of “following” links in microblogging networks. *IEEE Transactions on Knowledge and Data Engineering*, 27(8):2093–2106, 2015.
- Didier A Vega-Oliveros, Liang Zhao, and Lilian Berton. Evaluating link prediction by diffusion processes in dynamic networks. *Scientific reports*, 9(1):1–14, 2019.
- N Sumith, B Annappa, and Swapan Bhattacharya. Influence maximization in large social networks: Heuristics, models and parameters. *Future Generation Computer Systems*, 89:777–790, 2018.
- MEJ Newman. Network structure from rich but noisy data. *Nature Physics*, 14(6):542–545, 2018a.
- Manuel Gomez-Rodriguez, Jure Leskovec, and Andreas Krause. Inferring networks of diffusion and influence. *ACM Transactions on Knowledge Discovery from Data*, 5(4):1–37, 2012.
- Manuel Gomez-Rodriguez, Jure Leskovec, and Bernhard Schölkopf. Modeling information propagation with survival theory. In *International Conference on Machine Learning*, pages 666–674, 2013.
- Manuel Gomez Rodriguez, Jure Leskovec, David Balduzzi, and Bernhard Schölkopf. Uncovering the structure and temporal dynamics of information propagation. *Network Science*, 2(1):26–65, 2014.
- Maryam Ramezani, Hamid R Rabiee, Maryam Tahani, and Arezoo Rajabi. Dani: A fast diffusion aware network inference algorithm. *arXiv preprint arXiv:1706.00941*, 2017.
- Feng Ji, Wenchang Tang, Wee Peng Tay, and Edwin KP Chong. Network topology inference using information cascades with limited statistical knowledge. *Information and Inference: A Journal of the IMA*, 9(2):327–360, 2020.
- Hao Huang, Qian Yan, Ting Gan, Di Niu, Wei Lu, and Yunjun Gao. Learning diffusions without timestamps. In *Proceedings of the AAAI Conference on Artificial Intelligence*, volume 33, pages 582–589, 2019.
- Manuel Gomez Rodriguez, Jure Leskovec, and Bernhard Schölkopf. Structure and dynamics of information pathways in online media. In *Proceedings of the sixth ACM international conference on Web search and data mining*, pages 23–32, 2013.
- Maryam Tahani, Ali MA Hemmatyar, Hamid R Rabiee, and Maryam Ramezani. Inferring dynamic diffusion networks in online media. *ACM Transactions on Knowledge Discovery from Data*, 10(4):1–22, 2016.
- Jiin Woo, Jungseul Ok, and Yung Yi. Iterative learning of graph connectivity from partially-observed cascade samples. In *Proceedings of the Twenty-First International Symposium on Theory, Algorithmic Foundations, and Protocol Design for Mobile Networks and Mobile Computing*, pages 141–150, 2020.
- Sushrut Ghonge and Dervis Can Vural. Inferring network structure from cascades. *Phys. Rev. E*, 96:012319, 2017.
- M. E. J. Newman. Estimating network structure from unreliable measurements. *Phys. Rev. E*, 98:062321, 2018b.
- Zekarias T Kefato, Nasrullah Sheikh, and Alberto Montresor. Refine: representation learning from diffusion events. In *Machine Learning, Optimization, and Data Science: 4th International Conference, LOD 2018, Volterra, Italy, September 13-16, 2018, Revised Selected Papers 4*, pages 141–153. Springer, 2019.
- J. Wang, V. W. Zheng, Z. Liu, and K. C. Chang. Topological recurrent neural network for diffusion prediction. In *2017 IEEE International Conference on Data Mining*, pages 475–484, 2017.

- C. Yang, M. Sun, H. Liu, S. Han, Z. Liu, and H. Luan. Neural diffusion model for microscopic cascade study. *IEEE Transactions on Knowledge and Data Engineering*, pages 1–1, 2019.
- Yongqing Wang, Huawei Shen, Shenghua Liu, Jinhua Gao, and Xueqi Cheng. Cascade dynamics modeling with attention-based recurrent neural network. In *IJCAI*, pages 2985–2991, 2017.
- M. R. Islam, S. Muthiah, B. Adhikari, B. A. Prakash, and N. Ramakrishnan. Deepdiffuse: Predicting the 'who' and 'when' in cascades. In *2018 IEEE International Conference on Data Mining*, pages 1055–1060, 2018.
- Cheng Yang, Jian Tang, Maosong Sun, Ganqu Cui, and Zhiyuan Liu. Multi-scale information diffusion prediction with reinforced recurrent networks. In *Proceedings of the 28th International Joint Conference on Artificial Intelligence*, page 4033–4039. AAAI Press, 2019.
- Yansong Wang, Xiaomeng Wang, Yijun Ran, Radosław Michalski, and Tao Jia. Casseqgn: Combining network structure and temporal sequence to predict information cascades. *Expert Systems with Applications*, 206:117693, 2022a.
- Anis Najar, Ludovic Denoyer, and Patrick Gallinari. Predicting information diffusion on social networks with partial knowledge. In *Proceedings of the 21st International Conference on World Wide Web*, pages 1197–1204, 2012.
- Ling Sun, Yuan Rao, Xiangbo Zhang, Yuqian Lan, and Shuanghe Yu. Ms-hgat: Memory-enhanced sequential hypergraph attention network for information diffusion prediction. In *Proceedings of the AAAI Conference on Artificial Intelligence*, volume 36, pages 4156–4164, 2022.
- Mehrdad Farajtabar, Manuel Gomez Rodriguez, Mohammad Zamani, Nan Du, Hongyuan Zha, and Le Song. Back to the past: Source identification in diffusion networks from partially observed cascades. In *Artificial Intelligence and Statistics*, pages 232–240, 2015.
- Chaoyi Shi, Qi Zhang, and Tianguang Chu. Source estimation in continuous-time diffusion networks via incomplete observation. *Physica A: Statistical Mechanics and its Applications*, 592:126843, 2022.
- Shashidhar Sundareisan, Jilles Vreeken, and B Aditya Prakash. Hidden hazards: Finding missing nodes in large graph epidemics. In *Proceedings of the SIAM International Conference on Data Mining*, pages 415–423, 2015.
- Xueqin Chen, Fengli Zhang, Fan Zhou, and Marcello Bonsangue. Multi-scale graph capsule with influence attention for information cascades prediction. *International Journal of Intelligent Systems*, 37(3):2584–2611, 2022.
- Chunyu Yuan, Jiacheng Li, Wei Zhou, Yijun Lu, Xiaodan Zhang, and Songlin Hu. Dyhgcn: A dynamic heterogeneous graph convolutional network to learn users' dynamic preferences for information diffusion prediction. In *Machine Learning and Knowledge Discovery in Databases: European Conference, ECML PKDD 2020, Ghent, Belgium, September 14–18, 2020, Proceedings, Part III*, pages 347–363. Springer, 2021.
- Ding Wang, Lingwei Wei, Chunyu Yuan, Yinan Bao, Wei Zhou, Xian Zhu, and Songlin Hu. Cascade-enhanced graph convolutional network for information diffusion prediction. In *Database Systems for Advanced Applications: 27th International Conference, DASFAA 2022, Virtual Event, April 11–14, 2022, Proceedings, Part I*, pages 615–631. Springer, 2022b.
- Ruijie Wang, Zijie Huang, Shengzhong Liu, Huajie Shao, Dongxin Liu, Jinyang Li, Tianshi Wang, Dachun Sun, Shuochao Yao, and Tarek Abdelzaher. Dydiff-vae: A dynamic variational framework for information diffusion prediction. In *Proceedings of the 44th International ACM SIGIR Conference on Research and Development in Information Retrieval*, pages 163–172, 2021.
- Kazumi Saito, Ryohei Nakano, and Masahiro Kimura. Prediction of information diffusion probabilities for independent cascade model. In *International conference on knowledge-based and intelligent information and engineering systems*, pages 67–75. Springer, 2008.
- Myunghwan Kim and Jure Leskovec. The network completion problem: Inferring missing nodes and edges in networks. In *Proceedings of the SIAM International Conference on Data Mining*, pages 47–58, 2011.
- D. Rafailidis and F. Crestani. Network completion via joint node clustering and similarity learning. In *2016 IEEE/ACM International Conference on Advances in Social Networks Analysis and Mining*, pages 63–68, 2016.
- F. Masrour, I. Barjesteh, R. Forsati, A. Esfahanian, and H. Radha. Network completion with node similarity: A matrix completion approach with provable guarantees. In *2015 IEEE/ACM International Conference on Advances in Social Networks Analysis and Mining*, pages 302–307, 2015.
- Edo M Airoldi, David Blei, Stephen Fienberg, and Eric Xing. Mixed membership stochastic blockmodels. volume 21. Curran Associates, Inc., 2008.
- Zhiqiang Wang, Jiye Liang, and Ru Li. A fusion probability matrix factorization framework for link prediction. *Knowledge-Based Systems*, 159:72–85, 2018.

- Ece C Mutlu and Toktam A Oghaz. Review on graph feature learning and feature extraction techniques for link prediction. *arXiv preprint arXiv:1901.03425*, 2019.
- Aditya Krishna Menon and Charles Elkan. Link prediction via matrix factorization. In *Joint european conference on machine learning and knowledge discovery in databases*, pages 437–452, 2011.
- Dong Li, Yongchao Zhang, Zhiming Xu, Dianhui Chu, and Sheng Li. Exploiting information diffusion feature for link prediction in sina weibo. *Scientific reports*, 6:20058, 2016.
- Yan-Tao Jia, Yuan-Zhuo Wang, and Xue-Qi Cheng. Learning to predict links by integrating structure and interaction information in microblogs. *Journal of Computer Science and Technology*, 30(4):829–842, 2015.
- Hoi-To Wai, Yonina C Eldar, Asuman E Ozdaglar, and Anna Scaglione. Community inference from partially observed graph signals: Algorithms and analysis. *IEEE Transactions on Signal Processing*, 70:2136–2151, 2022.
- Minghu Tang. A joint weighted nonnegative matrix factorization model via fusing attribute information for link prediction. In *Mobile Multimedia Communications: 15th EAI International Conference, MobiMedia*, pages 190–205. Springer, 2023.
- Lang Chai, Lilan Tu, Xianjia Wang, and Juan Chen. Network-energy-based predictability and link-corrected prediction in complex networks. *Expert Systems with Applications*, 207:118005, 2022.
- Dongkwan Kim, Jiho Jin, Jaimeen Ahn, and Alice Oh. Models and benchmarks for representation learning of partially observed subgraphs. In *International Conference on Information and Knowledge Management (CIKM, Short Papers Track)*, 2022.
- Daniel D Lee and H Sebastian Seung. Algorithms for non-negative matrix factorization. In *Advances in neural information processing systems*, pages 556–562, 2001.
- Tinghui Zhou, Hanhuai Shan, Arindam Banerjee, and Guillermo Sapiro. Kernelized probabilistic matrix factorization: Exploiting graphs and side information. In *Proceedings of the SIAM international Conference on Data mining*, pages 403–414, 2012.
- Chain Monte Carlo. Markov chain monte carlo and gibbs sampling. *Lecture notes for EEB*, 581, 2004.
- Supplementary document proofs and details of paper. <https://github.com/maryram/DiffStru/blob/main/supplemental.pdf>, 2022.
- Nicholas G Polson, James G Scott, and Jesse Windle. Bayesian inference for logistic models using pólya–gamma latent variables. *Journal of the American statistical Association*, 108(504):1339–1349, 2013.
- Philipp Moritz, Robert Nishihara, Stephanie Wang, Alexey Tumanov, Richard Liaw, Eric Liang, Melih Elibol, Zongheng Yang, William Paul, Michael I Jordan, et al. Ray: A distributed framework for emerging {AI} applications. In *13th {USENIX} Symposium on Operating Systems Design and Implementation ({OSDI} 18)*, pages 561–577, 2018.
- Lada A Adamic and Eytan Adar. Friends and neighbors on the web. *Social networks*, 25(3):211–230, 2003.
- Qing Ou, Ying-Di Jin, Tao Zhou, Bing-Hong Wang, and Bao-Qun Yin. Power-law strength-degree correlation from resource-allocation dynamics on weighted networks. *Physical Review E*, 75(2):021102, 2007.
- Francois Lorrain and Harrison C White. Structural equivalence of individuals in social networks. *The Journal of mathematical sociology*, 1(1):49–80, 1971.
- Andrea Lancichinetti, Santo Fortunato, and Filippo Radicchi. Benchmark graphs for testing community detection algorithms. *Physical review E*, 78(4):046110, 2008.
- Nathan O Hodas and Kristina Lerman. The simple rules of social contagion. *Scientific reports*, 4:4343, 2014.
- Jure Leskovec, Lars Backstrom, and Jon Kleinberg. Meme-tracking and the dynamics of the news cycle. In *Proceedings of the 15th ACM SIGKDD international conference on Knowledge discovery and data mining*, pages 497–506, 2009.
- Marian-Daniel Iordache, José M Bioucas-Dias, and Antonio Plaza. Sparse unmixing of hyperspectral data. *IEEE Transactions on Geoscience and Remote Sensing*, 49(6):2014–2039, 2011.
- Brian W Matthews. Comparison of the predicted and observed secondary structure of t4 phage lysozyme. *Biochimica et Biophysica Acta (BBA)-Protein Structure*, 405(2):442–451, 1975.
- Laurens van der Maaten and Geoffrey Hinton. Visualizing data using t-sne. *Journal of machine learning research*, 9: 2579–2605, 2008.